RADC-TDR-63-349

HIGH POWER R-F WINDOW STUDY PROGRAM

QUARTERLY TECHNICAL NOTE NO. 4

1 April through 30 June 1963

VARIAN ASSOCIATES

PALO ALTO, CALIFORNIA

CONTRACT NO. AF 30(602)-2844

Prepared For

ROME AIR DEVELOPMENT CENTER

AIR FORCE SYSTEMS COMMAND

RESEARCH AND TECHNOLOGY DIVISION

UNITED STATES AIR FORCE

GRIFFISS AIR FORCE BASE

NEW YORK

VARIAN REPORT NO. 304—4Q

JULY 1963

DDC AVAILABILITY NOTICE

Qualified Requestors May Obtain Copies Of This Report From DDC

VARIAN associates
611 HANSEN WAY · PALO ALTO, CALIF.

RADC-TDR-63-349

HIGH POWER R-F WINDOW STUDY PROGRAM

QUARTERLY TECHNICAL NOTE NO. 4

1 April through 30 June 1963

VARIAN ASSOCIATES
Palo Alto, California

Contract No. AF 30(602)-2844
Project No. 5573
Task No. 557303

Prepared by: Floyd Johnson
Approved by: L. T. Zitelli
D. G. Dow

Prepared For

ROME AIR DEVELOPMENT CENTER
AIR FORCE SYSTEMS COMMAND
RESEARCH AND TECHNOLOGY DIVISION
UNITED STATES AIR FORCE
GRIFFISS AIR FORCE BASE
NEW YORK

VARIAN REPORT NO. 304-4Q

July 1963

Copy No. 25

ABSTRACT

The objective of specifying and deriving the elements of an equation for the analytical solution of waveguide window design problems has been met. By programming this equation and using dimension parameters as variables, a computer can be used to greatly speed up window design.

Two types of windows have been programmed and successfully computed. The block ceramic window, using dual-symmetric, inductive iris broadbanding techniques, has been computed for several cases and the results have been shown to be almost exact when compared to measured data. The thin disc type of window, either single or double disc dielectric cooled, has also been programmed. Comparisons of computed and measured results also show a very close correlation, but it is not so exact as for the block window. It is felt that the variations are due to propagation of high order modes and perhaps errors in the measured input data required in the latter solution.

The highest power attained to date on this study program was transmitted through a single disc, zero degree cut sapphire window. At a maximum ring circulating power of 275 kilowatts cw, the sapphire was tested for several hours without damage to, or failure of the window. The window was pressurized on both sides with approximately 35 psi of dry nitrogen gas. The metal-to-sapphire seal developed a small leak during the last test of the quarter after use in all of the windowtron tests.

Two identical double disc air cooled windows were tested to failure, which occurred in both cases at 100 kilowatts cw. The first failure was with pressurized nitrogen on both window faces and the second with a 10^{-6} Torr vacuum on one face. These failures were obviously caused by extremely high temperatures in the ceramic.

One FC75 fluid cooled window failed at 90 kilowatts cw which is half the power transmitted through a similar window during the second quarter. Power dissipation was also very much higher.

During the concluding test of the quarter a beryllium oxide half wavelength block window was tested to 170 kilowatts in the windowtron, at which point the vacuum was lost due to the leak in the sapphire window seal. Testing of this assembly will be resumed with a new windowtron.

This report also discusses cold test results on several windows which will be tested during the remaining quarter of this program.

Title of Report RADC-TDR-63-349

PUBLICATION REVIEW

This report has been reviewed and is approved. For further technical information on this project, contact Mr. Dirk Bussey, RALTP, Ext. 71286

Approved:

ARTHUR J. FROHLICH
Chief, Techniques Laboratory
Directorate of Aerospace Surveillance & Control

Approved:

WILLIAM T. POPE
Acting Director
Director of Aerospace Surveillance & Control

TABLE OF CONTENTS

LIST OF ILLUSTRATIONS

LIST OF ILLUSTRATIONS, (cont.)

SECTION I

OBJECTIVES OF PROGRAM

1-1. INTRODUCTION

This report is the fourth of four quarterly technical notes to be supplied to Rome Air Development Center, Griffiss Air Force Base, New York, by Varian Associates of Palo Alto, California, under United States Air Force Contract Number AF 30(602)-2844. At the end of the next quarter a final technical report will be prepared to conclude the program. This contract was awarded 6 July, 1962 in accordance with RADC Exhibit "A," dated 29 December 1961, and is entitled "High Power R-F Window Study."

1-2. OBJECTIVES

A. Primary

The objectives of the High Power R-F Window Study are to conduct theoretical and experimental investigations of methods for improving the average power transmission capabilities of high average power microwave tube windows. The ultimate objective is to design and test an X-band window to 250 kilowatts of c-w power. It is desirable that this window have a VSWR of less than 1.2 over a band of 25 per cent.

The general outline for this program included an investigation of various solid dielectrics and their adaptability and desirability for use with window configurations best suited for high average power transmission. Other phenomena believed to be responsible for window failure under the adverse operating conditions experienced in the field were also to be investigated. These include the effects of multipactor, strong magnetic fields, variations of gas pressure and the relative merits of various gaseous or liquid dielectrics used for cooling of window assemblies.

B. Fourth Quarter Objectives

The work scheduled for the fourth quarter placed major emphasis on high power testing of window assemblies in a windowtron and the continued fabrication of new windows. The windowtron is composed of two vacuum-tight windows connected by an r-f vacuum-tight, bakeable flange. The region between the windows is continuously pumped with a 5 liter VacIon® pump to maintain the vacuum, and the entire evacuated region is monitored visually through a single crystal transparent sapphire window. This window was scheduled to be tested separately in a nitrogen pressurized atmosphere to maximum power before use in the windowtron. The first double disc air cooled window was also tested in this manner.

With this latter window an evaluation of the effects of air cooling was to be made. Two assemblies of this type were fabricated and tested to failure under high power. Several other double disc FC-75 cooled windows made using both AL400 and AL300 ceramics were also scheduled for completion. However, because of unexpected difficulties in brazing vacuum-tight and FC-75 tight assemblies, only two were completed. One of these was tested to failure under high power. The other remains to be tested during the fifth quarter.

The windowtron was intended not only as a device to test windows under more nearly actual operating tube conditions, but as a means of experimenting with and investigating multipactor phenomena. No multipactor was seen to occur in any of the tests to date, and as yet no attempts have been made to induce it. It is hoped that time and circumstance will permit this phase of work during the next quarter.

In addition to the fabrication and testing portion of this study, the completion of computer programs for the analytic solution of both the thin disc type and the half-wavelength block windows was scheduled. This objective has been met, and the results appear to be as useful as expected, particularly with respect to the block window. It has been shown that the computer can predict almost exactly what bandwidth or impedance match can be expected of a given block window as a function of frequency. The solution for the thin disc type window also came close to actually measured results, but the accuracy was not as great. Detailed discussion appears in Section II.

SECTION II

TECHNICAL PROGRESS OF PROGRAM

2-1. GENERAL DISCUSSION

A. Conferences

Mr. Dirk Bussey, Rome Air Development Center's contract engineer, visited Varian Associates' laboratories in Palo Alto, California, on June 19th to appraise contractual progress and to discuss the work remaining for the final quarter of this contract.

B. Window Synthesis by Computer Solution

In order to eliminate many of the tedious, time consuming and expensive steps involved in designing high power waveguide windows, a method for designing them with the use of a computer was suggested and outlined.[1]

Briefly, a multiple matrix equation can be defined where each of its components is a discreet discontinuity or region which can be specified in terms of lumped impedances or admittances. It was shown that by using the transmission parameters of the resulting matrix product, the reflection coefficient or VSWR can be obtained as a function of frequency or any other variable as desired.

1. Block Windows

The first solution successfully run was for the beryllium oxide half wavelength window discussed in the third technical note.[2] Computing a theoretical solution for this particular window provided a good check on the predictability of the window match.

A sketch showing the actual dimensions of the assembly as it was tested is shown in Figure 1(a) and a sketch of the model is shown in Figure 1(b). The transmission parameter matrix, T^a, is due to a symmetric inductive iris. The equation for this shunt element is readily available in several references[3,4] and is

$$\frac{B}{Y_o} = -j\frac{\lambda g}{a}\cot^2\frac{\pi d}{a}\left\{1+\frac{3}{4}\left[\frac{1}{\sqrt{1-\left(\frac{2a}{3\lambda}\right)^2}}-1\right]\sin^2\frac{\pi d}{a}\right\}^{-1} \qquad (1)$$

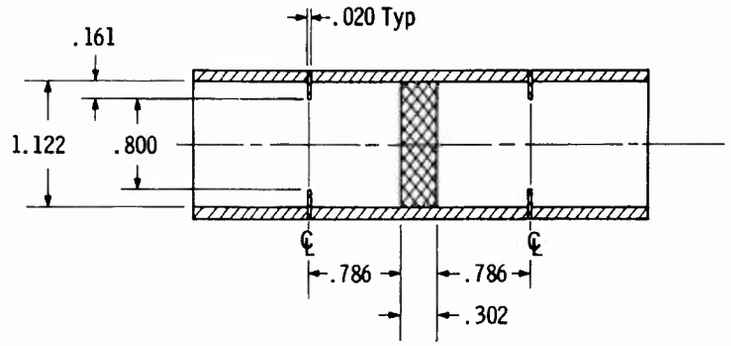

(a) Actual BeO Block Window Dimension

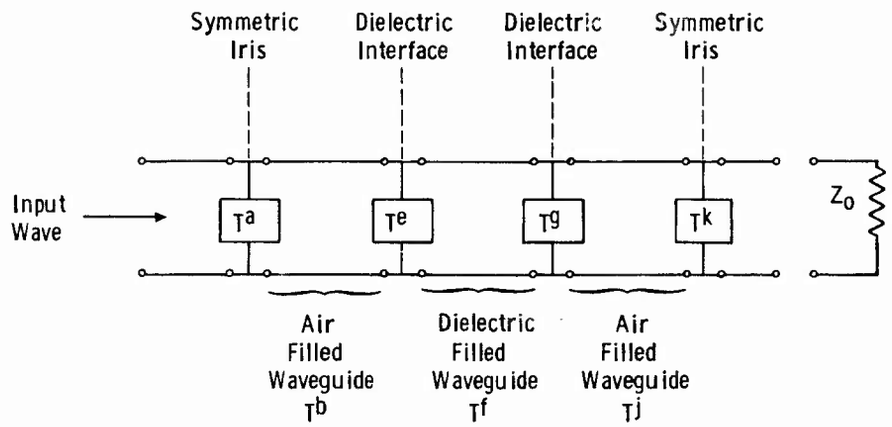

(b) BeO Block Window Model

FIGURE 1
BERYLLIUM OXIDE WINDOW ACTUAL AND COMPUTER MODELS

where

a = waveguide width

λg = waveguide wavelength

λ = free space wavelength

d = distance separating inside edges of iris pair

When used with the definition[5] for the transmission parameters of a shunt element, T^a is

$$T^a = \begin{bmatrix} 1 - \frac{B}{2Y_o} & -\frac{B}{2Y_o} \\ \frac{B}{2Y_o} & 1 + \frac{B}{2Y_o} \end{bmatrix}$$

T^k is defined similarly.

It has been shown[1] that for a dielectric loaded waveguide, whether air or ceramic filled, the transmission parameter matrix is

$$T = \begin{bmatrix} e^{-j\beta L} & 0 \\ 0 & e^{j\beta L} \end{bmatrix}$$

where

$$\beta = \frac{2\pi}{\lambda}\left[\epsilon_R - \left(\frac{\lambda}{2a}\right)^2\right]^{1/2} \quad (TE_{10}\ \text{MODE})$$

and L = the length of the guide section. The magnitude of β is calculated by the computer given the proper values of input data such as the relative dielectric constant, ϵ_R, etc.

It has also been shown[1] that the matrix for a dielectric interface has the form

$$T = \begin{bmatrix} \frac{1+R}{2} & \frac{1-R}{2} \\ \frac{1-R}{2} & \frac{1+R}{2} \end{bmatrix}$$

where

$$R = \frac{Z_{01}}{Z_{02}} = \frac{\lambda g_1}{\lambda g_2} = \left[\frac{\epsilon_2 \left(\frac{\lambda}{2a}\right)^2}{\epsilon_1 - \left(\frac{\lambda}{2a}\right)^2} \right]^{1/2} \qquad (TE_{10} \text{ MODE})$$

A complete listing of the entire program, as well as an explanation of some of the symbols used to identify the variables shown in the above equations, is presented in the Appendix. However, no attempt is made to explain the intricacies of the Fortran language.

The characteristic VSWR curves for the beryllium oxide window of this example are shown in Figures 2 and 3. The unbrazed cold test curve made on this window with moveable irises is shown in comparison with the computed results in Figure 2. The curves are not exactly alike, but considering that tolerance build up and unsoldered joints could cause several deviations from the ideal case, it would seem that the computed results are very good.

Figure 3 illustrates the VSWR curve of the completed vacuum-tight window which was tested in the resonant ring. The dimensions of this window varied slightly from the ideal case and are shown in the sketch of Figure 4. Another factor which could cause considerable variation from the computed results is small deviations in the ceramic dielectric constant.

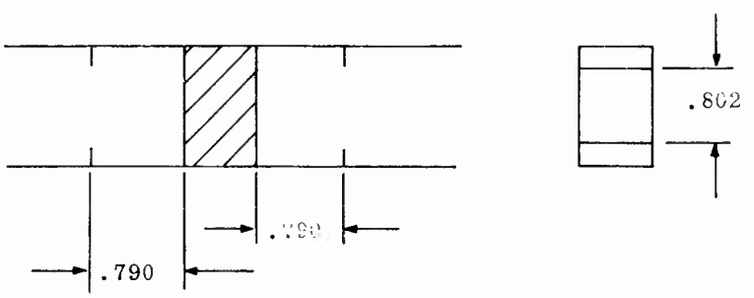

FIGURE 4
VACUUM-TIGHT BERYLLIUM OXIDE WINDOW DIMENSIONS

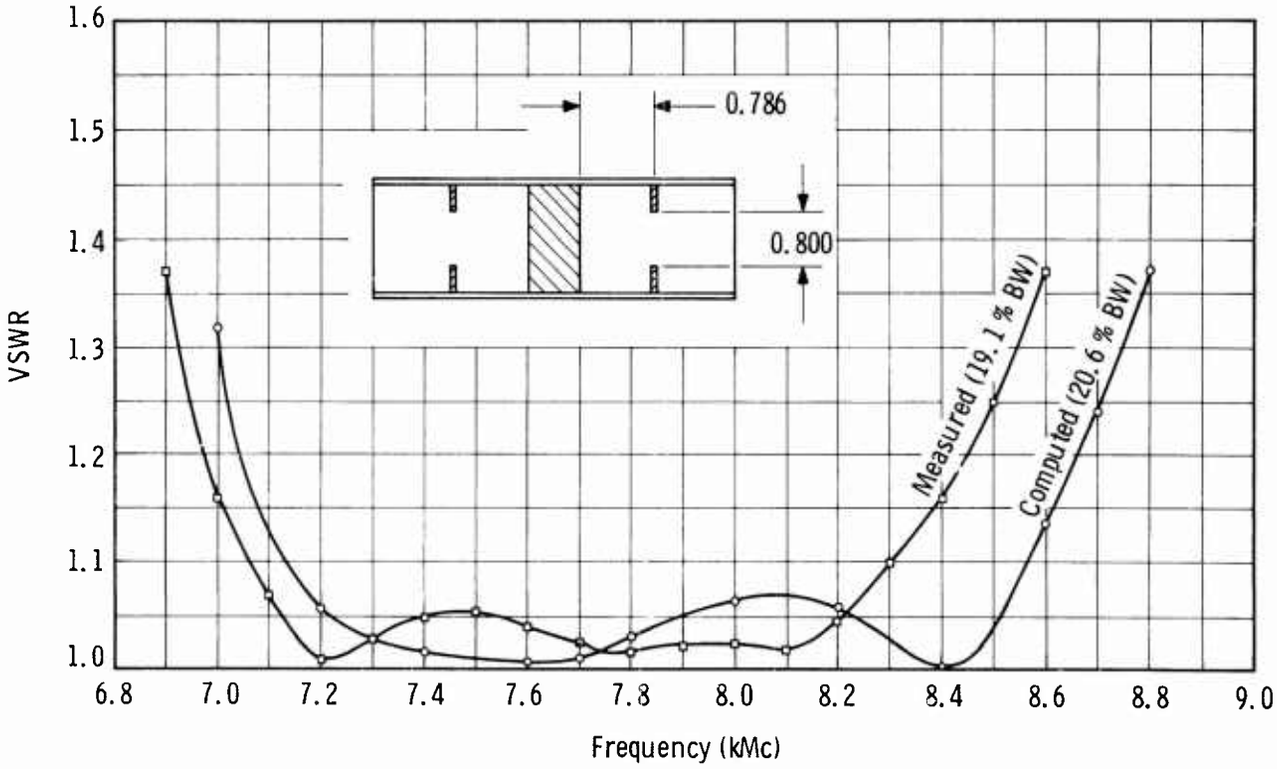

FIGURE 2
MEASURED AND COMPUTED RESULTS FOR BROADBAND
BERYLLIUM OXIDE WINDOW

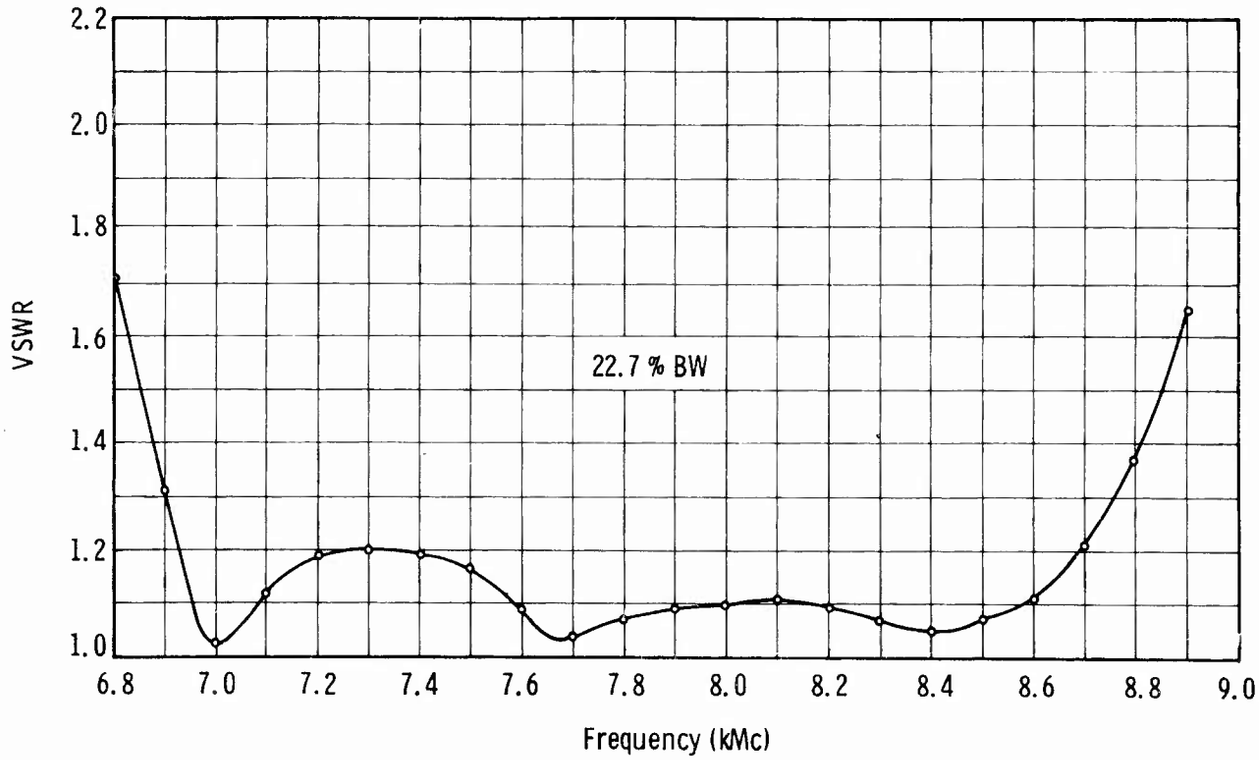

FIGURE 3
VACUUM-TIGHT BERYLLIUM OXIDE
WINDOW CHARACTERISTICS

Figure 5 illustrates the usefulness of the computer solution in another way. Here is shown the effect of varying the dimension parameters by means of a "DO LOOP" within the program. The iris gap width is varied over a plus and minus range with a resulting variation in the impedance match. Any or all of the dimensions can be similarly varied over a range to establish where the very broadest bandwidth possible can be obtained.

Hand plotting of these curves can be eliminated by feeding the computer output to a subroutine which will give an automatic print out of all curves. A typical computer run for this program using the IBM 7094 machine takes .02 to .04 hours at the current service organization rate of $575 per hour. By varying several dimension parameters within one given run, up to 200 variations of a window design have been obtained for less than $25.

Other information easily extracted from such a computer run is the actual susceptance value of the irises used and the thickness of the block window at each frequency. Figure 6 gives the block size as a function of frequency for beryllium oxide with relative dielectric constant of 6.5 and is useful for quick reference in design work.

2. Disc Windows

Toward the end of the third quarter of this contract, initial results from the computer solution for the thin disc windows were obtained. It was indicated in the third technical note[6] that an error existed either in the measurement of the abrupt transition impedances or in the mathematical model.

During this reporting period it was determined that the error was in the method of measurements specifying the transmission parameter matrix for the window input and output transitions. The method used, as discussed, was rather devious and it is recommended that the method given by Storer, et al.[7] be used. These measurements are time consuming, when done over a wide frequency band, but they need only be done once for any given size of transition and can be used repeatedly in similar designs.

The values for the 1.4-inch to WR112 transition scattering coefficients are given in Figure 7. These were measured using the techniques referenced above and averaged according to the semiprecision procedures defined by Felsen and Oliner.[8] The measured data are plotted and a smooth curve is drawn through the points. The actual values of coefficients used are those read from the smooth curve so that no single point of measured data can affect the final results in an inordinate manner.

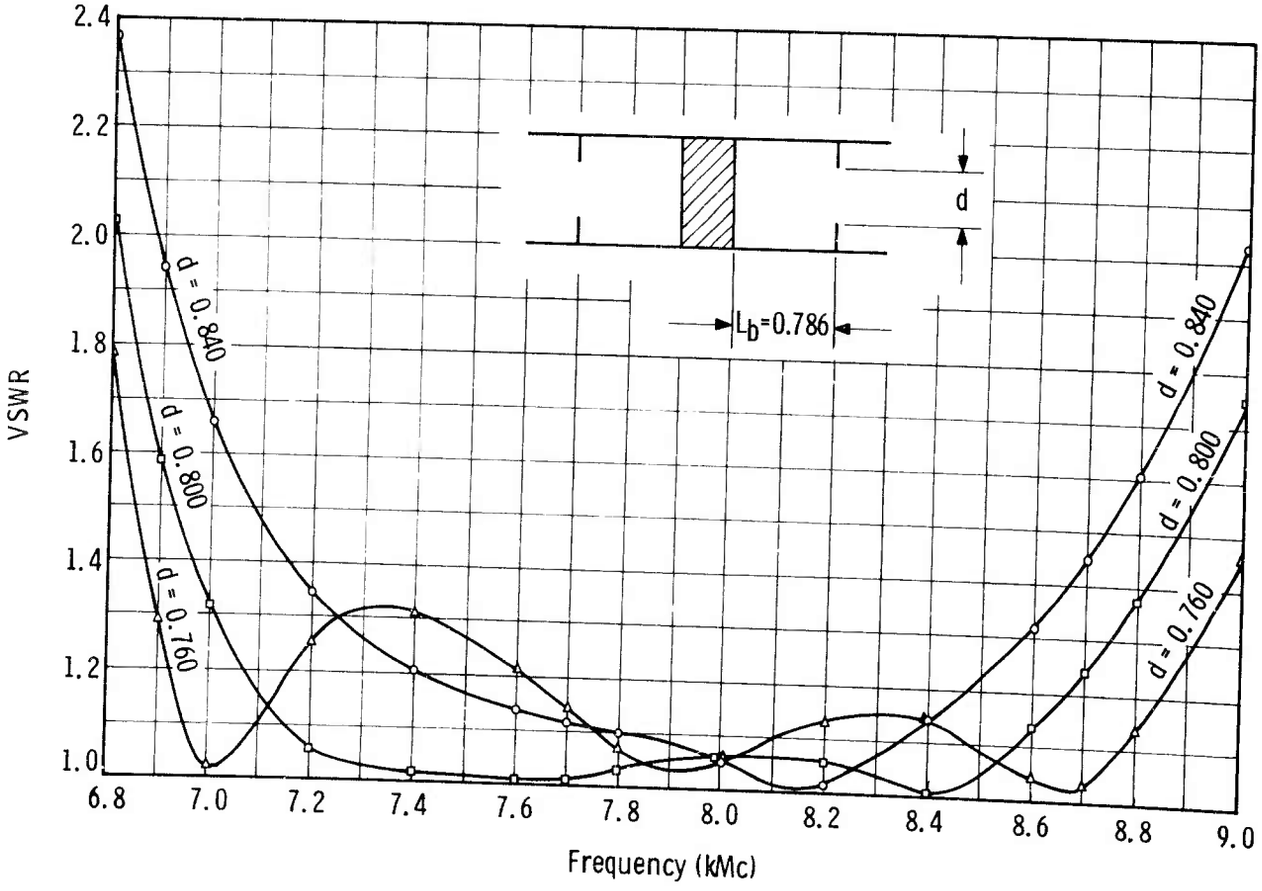

FIGURE 5
BeO BLOCK WINDOW COMPUTER RESULTS SHOWING
EFFECT OF VARIATION IN IRIS SIZE

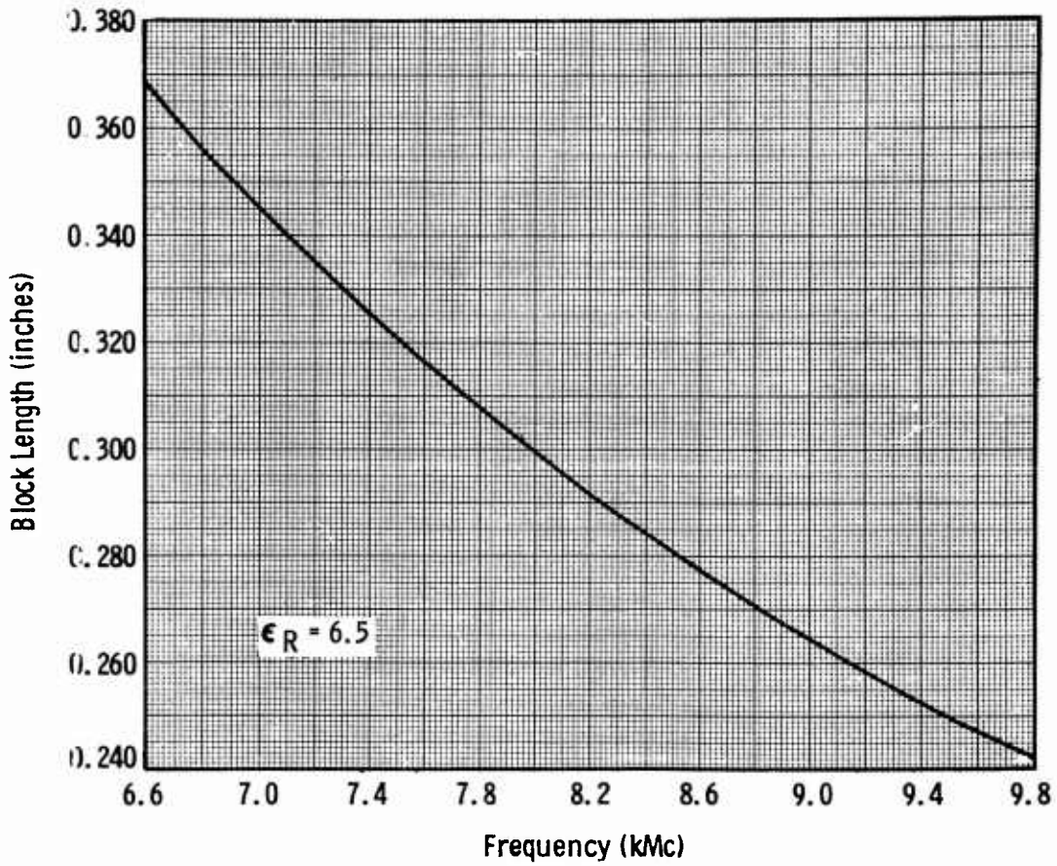

FIGURE 6
BERYLLIUM OXIDE HALF-WAVELENGTH BLOCK SIZE
CHART FOR WR112 WAVEGUIDE

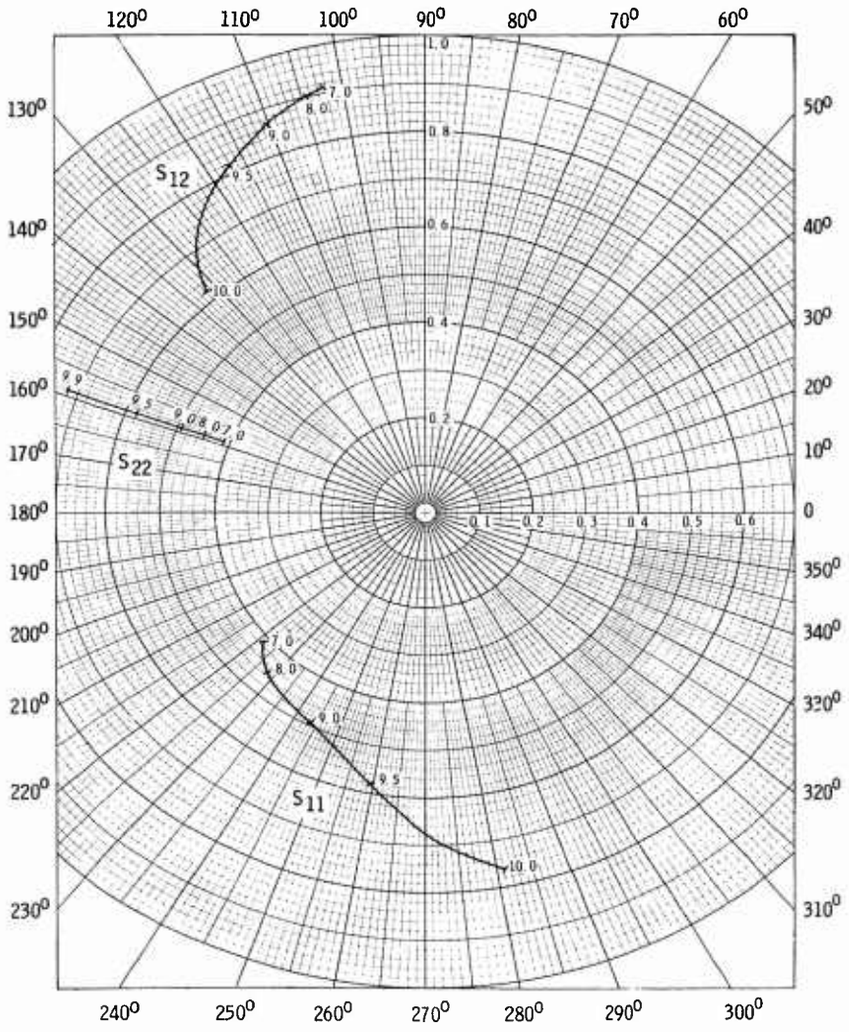

FIGURE 7
SCATTERING MATRIX COEFFICIENT VALUES FOR 1.4-INCH DIAMETER TO WR112 WAVEGUIDE TRANSITION

These data are then fed into the computer with T^a and T^k being defined as

$$T_{11}{}^a = S_{12} - \frac{S_{11} S_{22}}{S_{12}} = T_{11}{}^k$$

$$T_{12}{}^a = \frac{S_{22}}{S_{12}} = - T_{21}{}^k$$

$$T_{21}{}^a = - \frac{S_{11}}{S_{22}} = - T_{12}{}^k$$

$$T_{22}{}^a = \frac{1}{S_{12}} = T_{22}{}^k$$

The curves for a typical thin disc window with abrupt WR112 to circular waveguide transitions were computed. One comparison between measured and computed data is shown in Figure 8. The actual curve shows a sharp resonant mode spike at 9.2 kMc and then falls again to a low value of VSWR, whereas the computed curve shows a continual rise in VSWR at that frequency. Agreement between results to that point is reasonably good and the best explanation of the divergence at the higher end of the frequency band is that the cylindrical section of waveguide is propagating in a TM mode.[9] Although the TM_{11} mode is cut off at 10270 Mc in this size waveguide, the fact that the guide is partially dielectric filled probably lowers the cutoff frequency.

Propagation of this mode, of course, is very undesirable because it would be accompanied by normally directed electric fields at the face of the window itself. Multipactor could result and concentration of transmitted power density at the two off-center nodes characteristic of this mode would cause premature failure of the dielectric. Several thin disc windows have failed from what appears to be overheating in two regions just above and below the axis of the cylinder as sketched in Figure 9.

To test the validity of the computer solution further, preliminary tests were made on a full wavelength long thin disc window. There were two reasons for doing this.

A full wavelength window would reduce the possibility of transmission of the TM or other higher order modes. Also, it was felt that the proximity of the ceramic to the abrupt transitions would cause error to be introduced in the computed

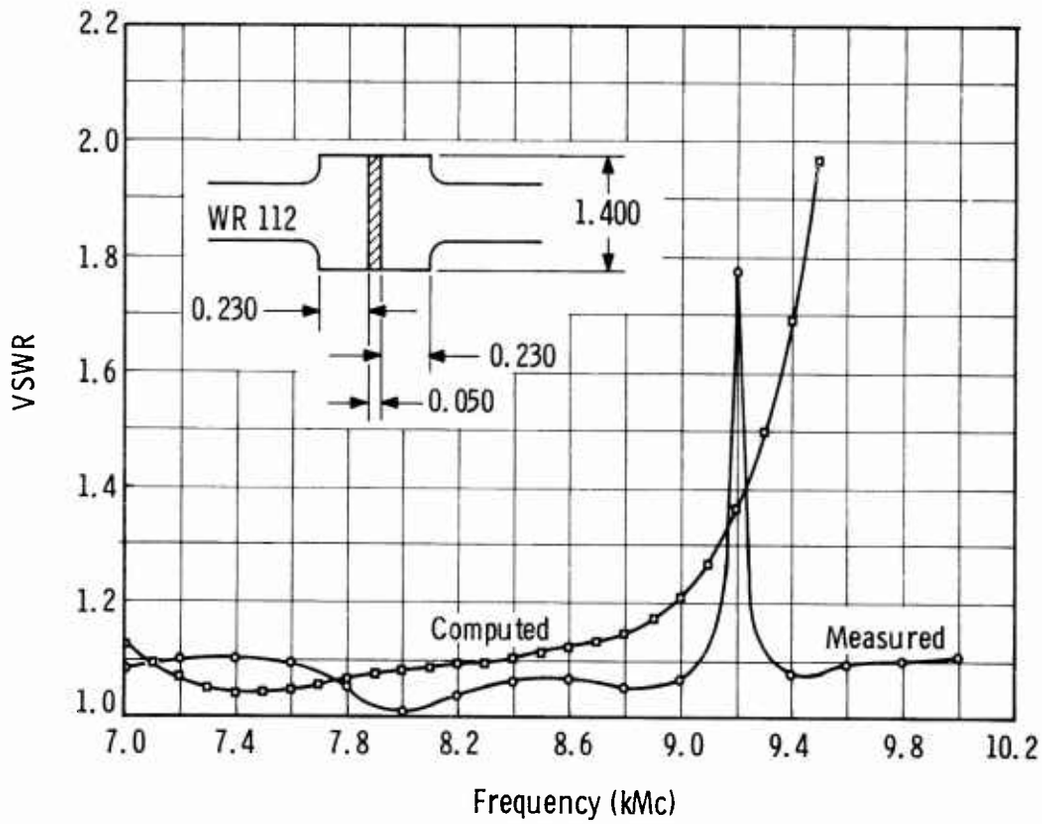

FIGURE 8
COMPUTED AND MEASURED VSWR CHARACTERISTICS OF A
SYMONS-TYPE SINGLE DISC AL300 WINDOW

solution because of fringing field effects during the transition from the TE_{10}^{o} to TE_{11}^{o} modes. Of course, the increased length would decrease the bandwidth and this is just what happened (see Figure 10).

These curves illustrate measured and computed results for the same window, where the computed result was selected from several to conform as near as possible to measured one. The difference in the two models is 0.080 inch in the space between window face and transition. The calculated result was obtained using $L_b = 1.040$ inches where L_b was 0.960 inch in the actual window. This represents an error of less than 8 per cent. Despite the error the solution is useful and further work may reveal where the error lies and effect its removal.

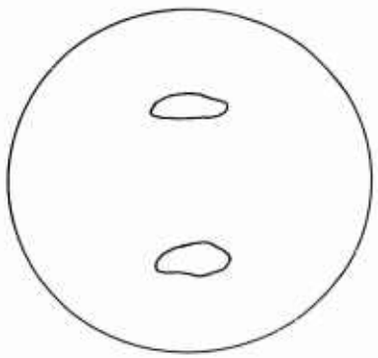

FIGURE 9
ILLUSTRATION OF CERAMIC FAILURE DUE TO
TRANSMISSION OF TM11 MODE

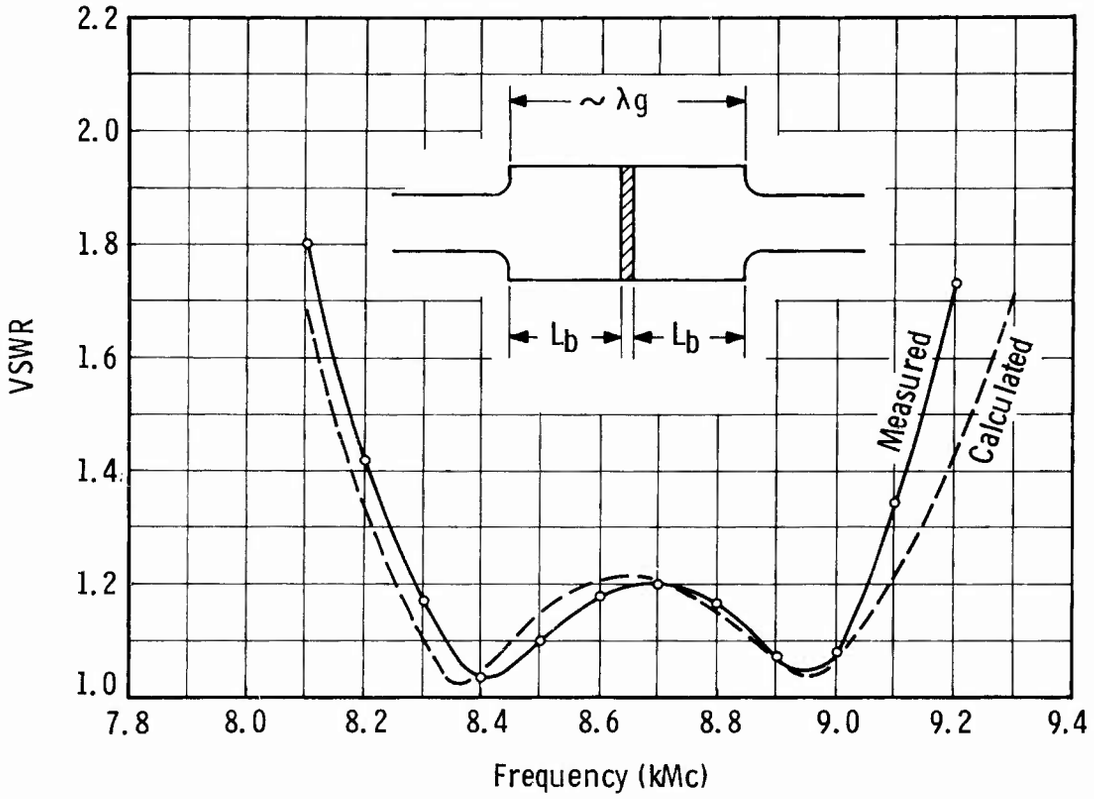

FIGURE 10
COMPUTED AND MEASERED VSWR CHARACTERISTICS OF
A THIN DISC λg LONG, CYLINDRICAL WINDOW

2-2. WINDOW CONSTRUCTION AND HIGH POWER TESTING

A. Single Disc Alumina Windows

Until this time during this window study no effort has been directed to building and testing the conventional Symons-type single thin disc window using ordinary aluminum oxide. There are two reasons for pursuing this objective now.

As discussed in the window synthesis section of this report, the TM modes are more likely to propagate when the diameter of the cylinder is large. It follows that a reduction in diameter would move the cutoff frequencies of these modes to a higher frequency, decreasing the likelihood of breakdown.

The cost of single crystal zero degree cut sapphire discs can be reduced 25 to 35 per cent by decreasing the diameter from 1.4 inches to 1.250 inches. The latter size sapphire discs are also more readily available. One more factor influenced the decision to test 1.250-inch diameter AL300 windows. In the preparation of the sapphire for brazing vacuum-tight assemblies, new molybdenum keepers, stainless steel spaces, etc., had to be prepared. To test these new parts for exact dimension change under high temperature brazing conditions, relatively cheap alumina discs were used. At this time two each of the sapphire and AL300 windows are vacuum tight and are being prepared for final brazing to waveguide sections.

The cold test results for the AL300 window are shown in Figure 11. The bandwidth under 1.2 VSWR, as shown, is very large and in fact is under 1.07 for the entire 7.05 to 10.0 kMc, WR112 frequency range. Unfortunately resonant ghost modes interrupt this bandwidth at various intervals. These modes have been identified by needle perturbation techniques as being the TE_{111}^{o}, TM_{010}^{o}, TE_{211}^{o} - TM_{111}^{o} and TE_{311}^{o} arranged in ascending order of frequency. The TE_{111}^{o} mode is the orthogonal counterpart of the TE_{11}^{o} transmission mode and is very easily excited by any disymmetry in the waveguide. The TM_{010}^{o} mode is loosely coupled and often is difficult to excite. The TE_{211}^{o} - TM_{111}^{o} modes are degenerate (both exist at the same frequency) and are the hardest modes to excite. They are not normally excited in thin disc windows. The last mode, the TE_{311}^{o}, tends to be the most strongly excited one and has the most pronounced effect on the reflected power. Since it always exists at the high end or beyond the high end of the band in normally used waveguide diameters, its presence can usually be disregarded.

High power windowtron tests will proceed on at least two assemblies of this type during the next quarter.

B. Single Thin Disc Sapphire Windows

The 1.4-inch diameter single crystal, zero degree cut synthetic sapphire window reported on in the previous quarter was tested in several different ways during this reporting period.

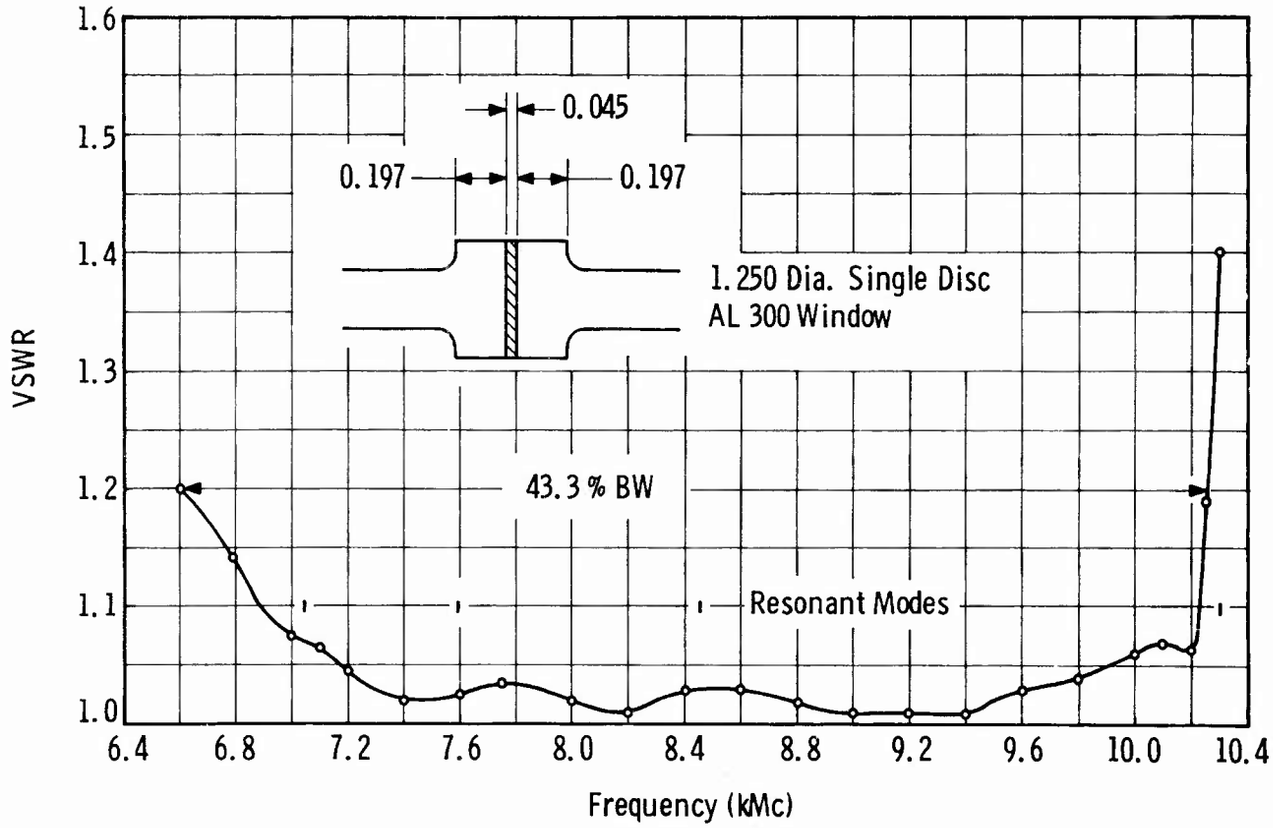

FIGURE 11
SINGLE DISC AL300 VSWR CHARACTERISTICS

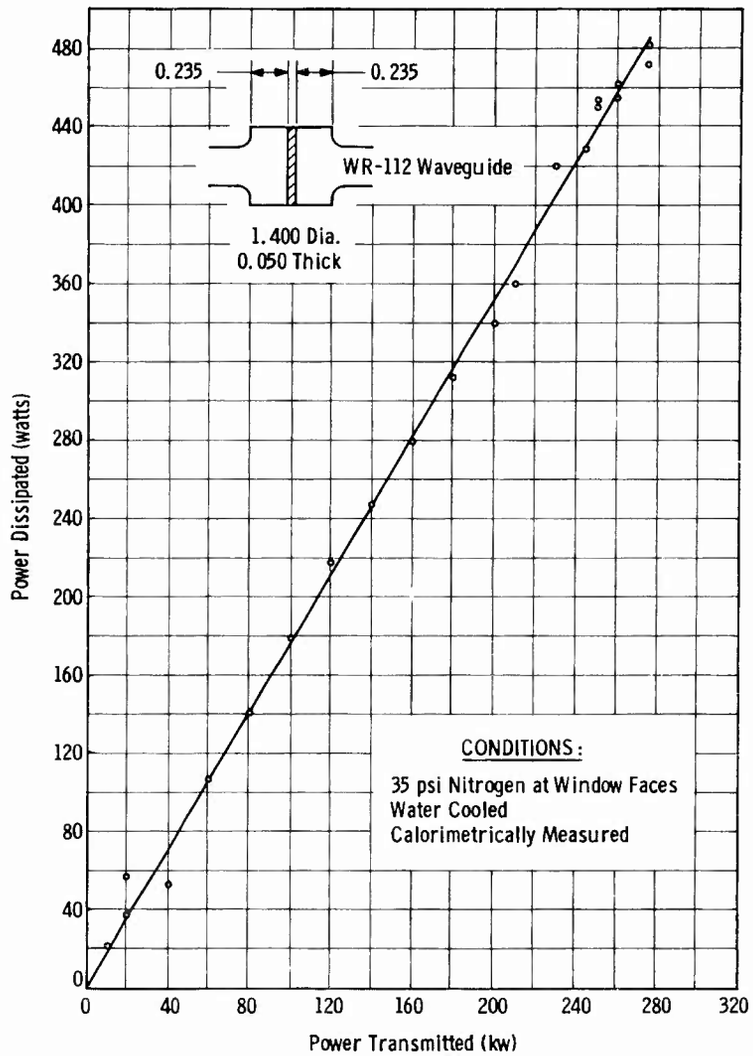

FIGURE 12
POWER DISSIPATION IN A SINGLE CRYSTAL ZERO DEGREE CUT SAPPHIRE SYMONS-TYPE WINDOW

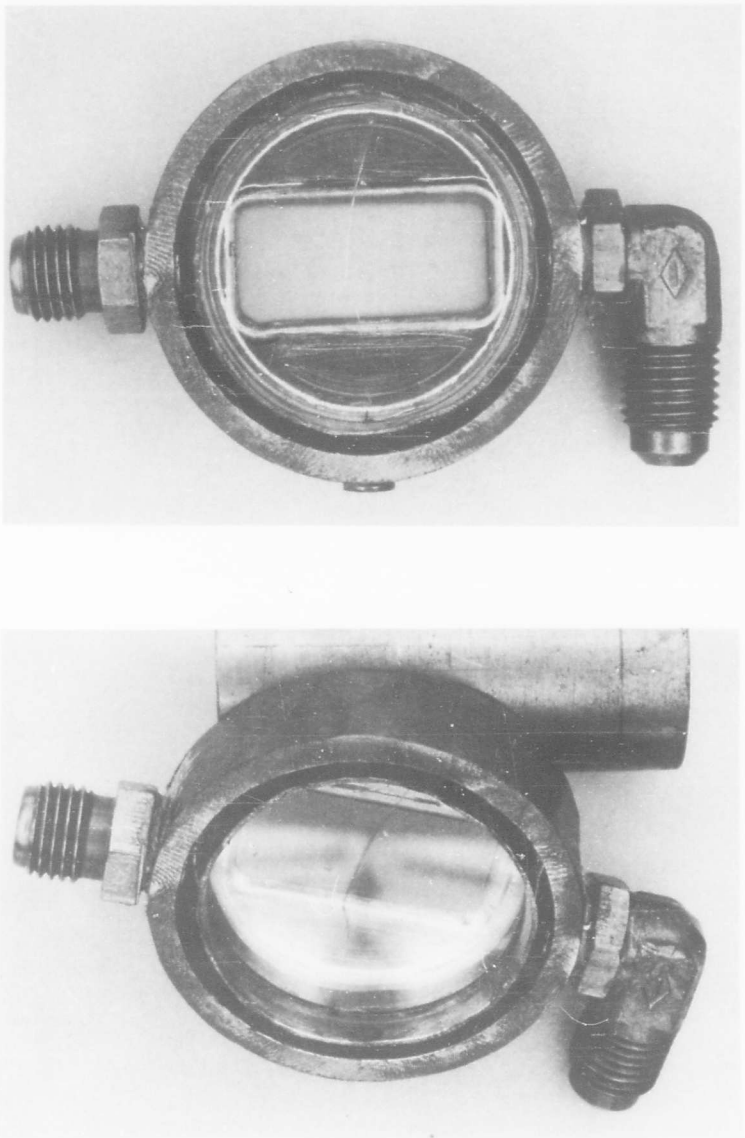

FIGURE 13
DISASSEMBLED SAPPHIRE WINDOW SHOWING
POINT OF SEAL FAILURE

First, in order to get a good comparison between high power tests previously performed with windows pressurized on both sides, this window was also pressurized to 35 psi of nitrogen. Power was increased in 20 kw increments and allowed to remain at each new level for periods up to one-half hour. Calorimetric measurements of power dissipation were made and are shown in Figure 12. The maximum power transmitted through the window was 275 kilowatts cw over a period of about three hours. Tests were discontinued at this power level because no additional ring drive power was available.

The very satisfactory performance of this window allowed its use as part of the high vacuum testing windowtron. All the windowtron tests performed and yet to be described were made with this window. During the last of these, while testing this window in series with the broadband beryllium oxide assembly, a very small leak developed at one point in the sapphire disc-to-metal seal. There had been no visible damage to the sapphire itself. During subsequent removal of the waveguide sections, the sapphire disc cracked across its diameter beginning at the point which appears to be a small burned area on the power input, pressurized side of the window as shown in the photographs of Figure 13. Closer inspection of this region showed a very slightly pitted hemisphere about 0.010 inch in radius on the copper immediately adjacent to the sapphire.

Assuming the crack's position is not just a coincidence, it could be concluded that a small strain developed in the sapphire in this plane. A sketch of the crystal structure (Figure 14) shows that the crack is not in the direction of any of the crystal stress boundaries previously photographed.[10]

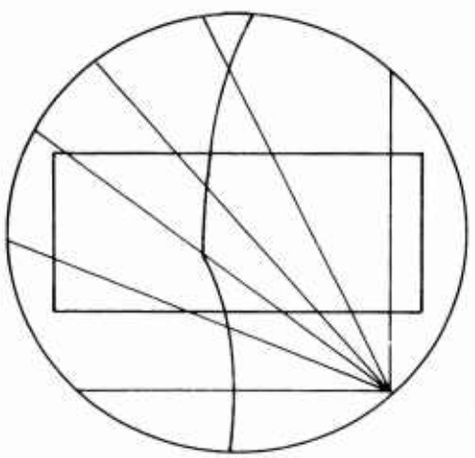

FIGURE 14
SKETCH OF SAPPHIRE WINDOW SHOWING STRESS BOUNDARIES AND CRACK ORIENTATION

Because this vital half of the windowtron failed, tests have been temporarily halted. Additional disc sapphire windows were already in the process of being fabricated, however, and no further delay is anticipated. The new 1.250-inch diameter sapphire windows will have dimensions identical to that of the single disc alumina versions discussed in the previous section. The VSWR characteristics can be seen in Figure 15. These, too, are very similar in every respect to the alumina window.

C. Double Thin Disc Windows

1. Aluminas

Two double disc, conical transition-type windows were tested under high power during the third quarter. Both failed at identically the same power level, 100 kilowatts, although the test conditions were not identical.

The first one was to be tested with pressure on both input and output power sides of the window. Again this was planned in order to make performance comparisons between this window and all the other windows similarly tested.

The experimental procedure decided upon was to increase the power level slowly to 100 kilowatts cw with stationary air between the discs, and at the same time measure the power dissipation in the water-cooled window jacket. Once at the 100 kw level, the procedure was to have been repeated with clean high pressure air or nitrogen blowing across the inside faces of the discs, again repeating the dissipation measurements. This procedure would give a fairly accurate measure of the effectiveness of air cooling waveguide windows.

After attaining the 100 kw level for several minutes, however, the window unmistakably failed. Both ceramic discs cracked simultaneously, one of them obviously because of over heating. The melted remains of both discs of this window are shown in the photograph of Figure 16. Note particularly that the major portion of the shattered effect resulted from removing the window from the waveguide sections. The dissipation curve is shown in Figure 17.

The failure of this window at such a low power level was very disappointing when viewed in the light of the several considerations that went into its design.[11] The first reaction was that perhaps it had been an accident. Hence, a more cautious implementing of a similar test procedure was followed for another identical window.

The waveguide on either side of the window cylinder was cooled by water and heat dissipation monitored constantly. At each new power level, measurements were made of the heat dissipation in the water jacket with and without a high pressure nitrogen flow between the dual discs. In this way the amount of heat carried away by the gas was separated out from the amount carried away by the water.

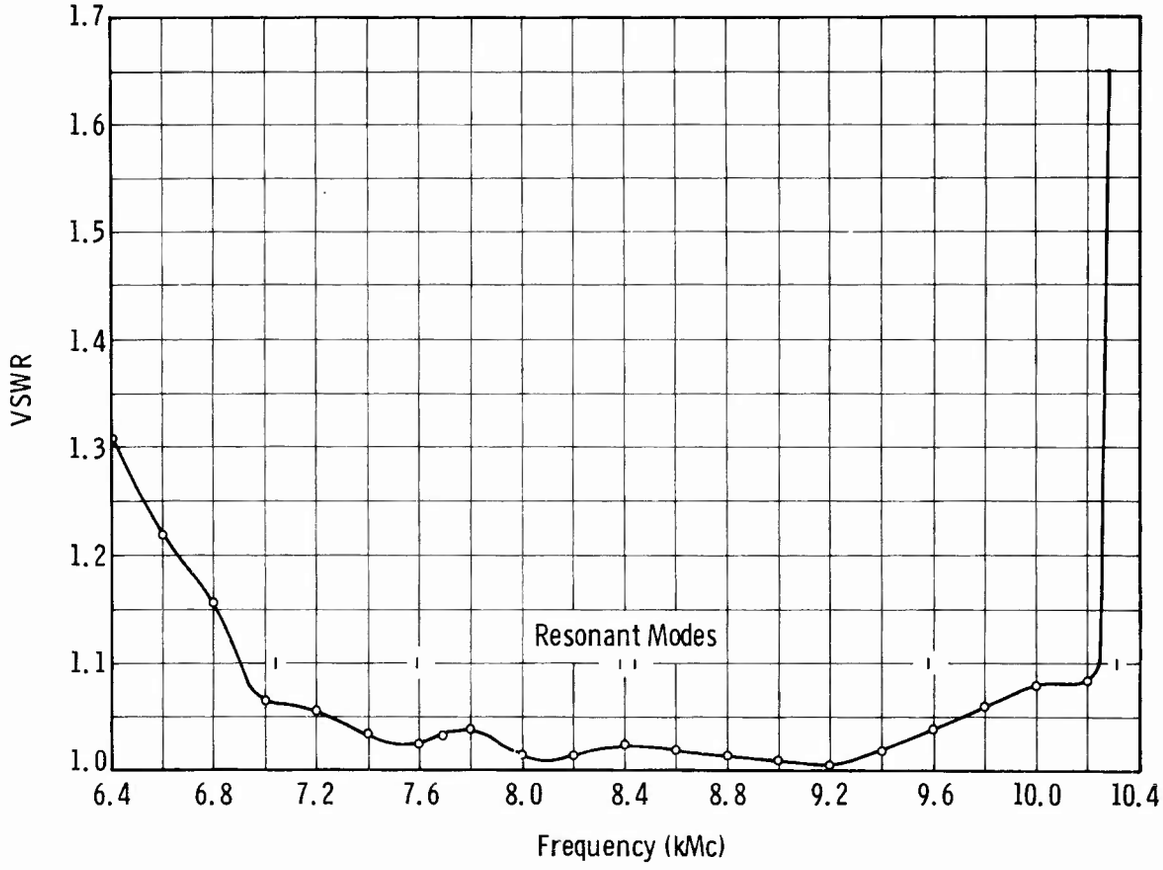

FIGURE 15
SINGLE DISC SAPPHIRE VSWR CHARACTERISTICS

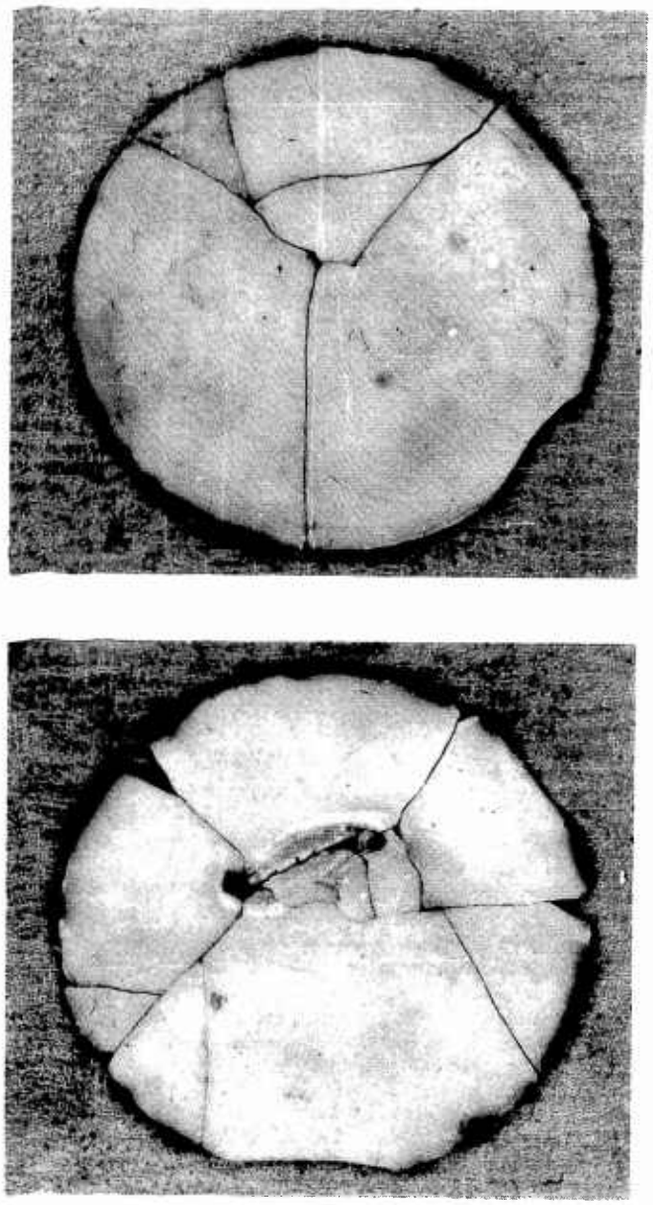

FIGURE 16
DISASSEMBLED DOUBLE DISC WINDOW NO. 1 CERAMICS
SHOWING HIGH TEMPERATURE FAILURE

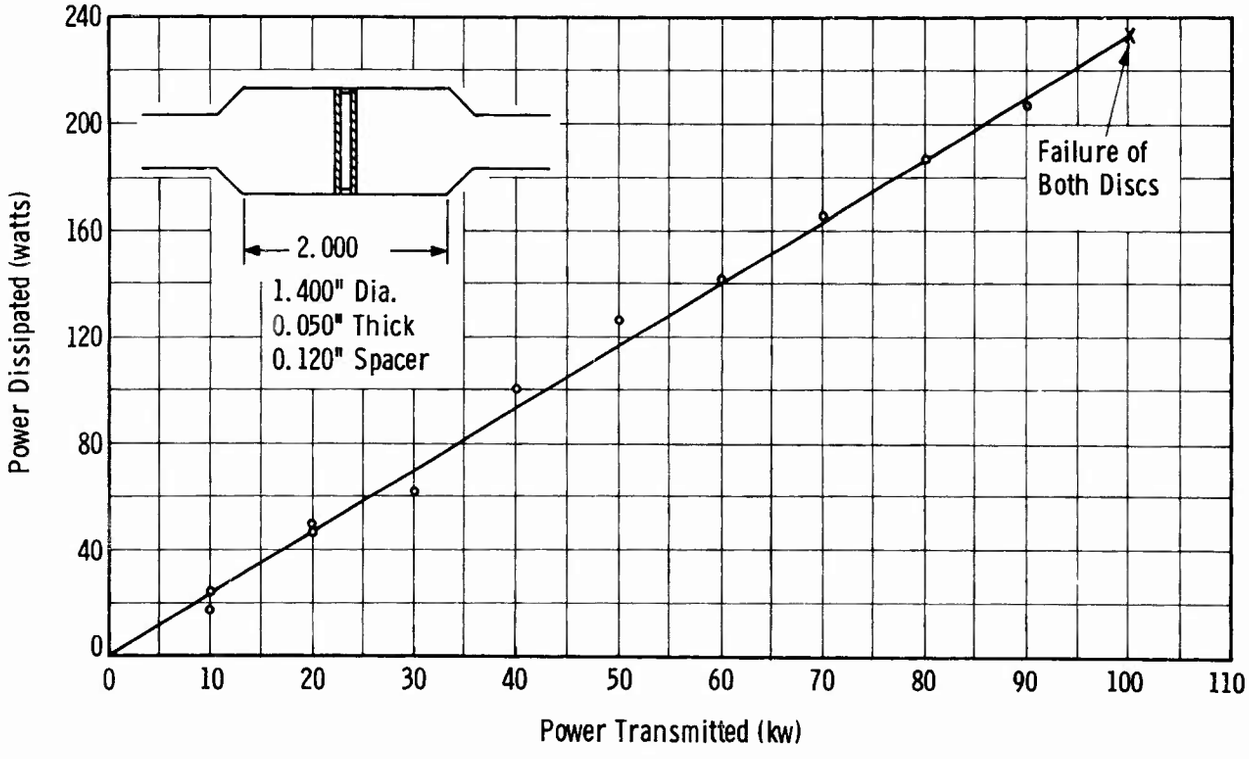

FIGURE 17
POWER DISSIPATION IN DOUBLE DISC AL300 WINDOW NO. 1

Figure 18 shows that about 10 to 12 per cent of the heat was removed by the air. Obviously this method of cooling is not nearly as effective as it needs to be, because the window also failed at 100 kw.

One additional difference existed in this test compared to any of the previous ones. A vacuum of 10^{-6} Torr was maintained on one face of the window with power being transmitted from the vacuum side through the window to the pressurized side. The evacuated region was viewed through the transparent sapphire disc. At the power level attained, no multipactor or arcing was seen. Very small hot spot specks were seen in the AL300 discs at the higher power levels. Random points in the evacuated region which were probably pieces of lint or dust also glowed even at low power levels like 10 kw. The vacuum side window failed as shown in Figure 19, but the pressurized side was undamaged.

No further tests on this type of window are planned during the remainder of this program. This is warranted because of the relatively low average power level at which failure occurs. The conical transition window may have possibilities when made with sapphire discs or used with high peak power pulsed systems. However, these aspects do not fall within the scope of this program.

Fabrication and testing of double disc FC75 cooled windows were resumed during this quarter. One assembly, very similar to the assembly tested to 180 kilowatts, [12] failed at 90 kilowatts. This window has been improved by thickening the discs by about 17 per cent, which would theoretically increase the fracture pressure by 36 per cent.

This failure is considered to be very premature. The power dissipation curve of Figure 20 shows that 12 watts were dissipated per kilowatt transmitted, whereas the previous window dissipated 7.5 watts per kilowatt. No good reason exists for this difference. Photographs of the failure (Figure 21) show two very heavily melted areas on the power output window, while the power input side (bottom) is still vacuum-tight. Chemical analysis of the very hard glassy deposits seen up to 20 inches away from the window and down the waveguide after the failure showed a predominance of silicon, aluminum and magnesium. The appearance of the deposits and the constituents indicate a very high temperature was obtained near the window.

Since this type of window can be broadbanded over such a wide mode-free region, further testing of more assemblies is planned. Some difficulties have been experienced in brazing vacuum-tight windows and are largely due to the multiple braze runs required to mount the strengthening hoops. Five more double disc alumina windows are in preparation for test, two of which will not have the strengthening hoops.

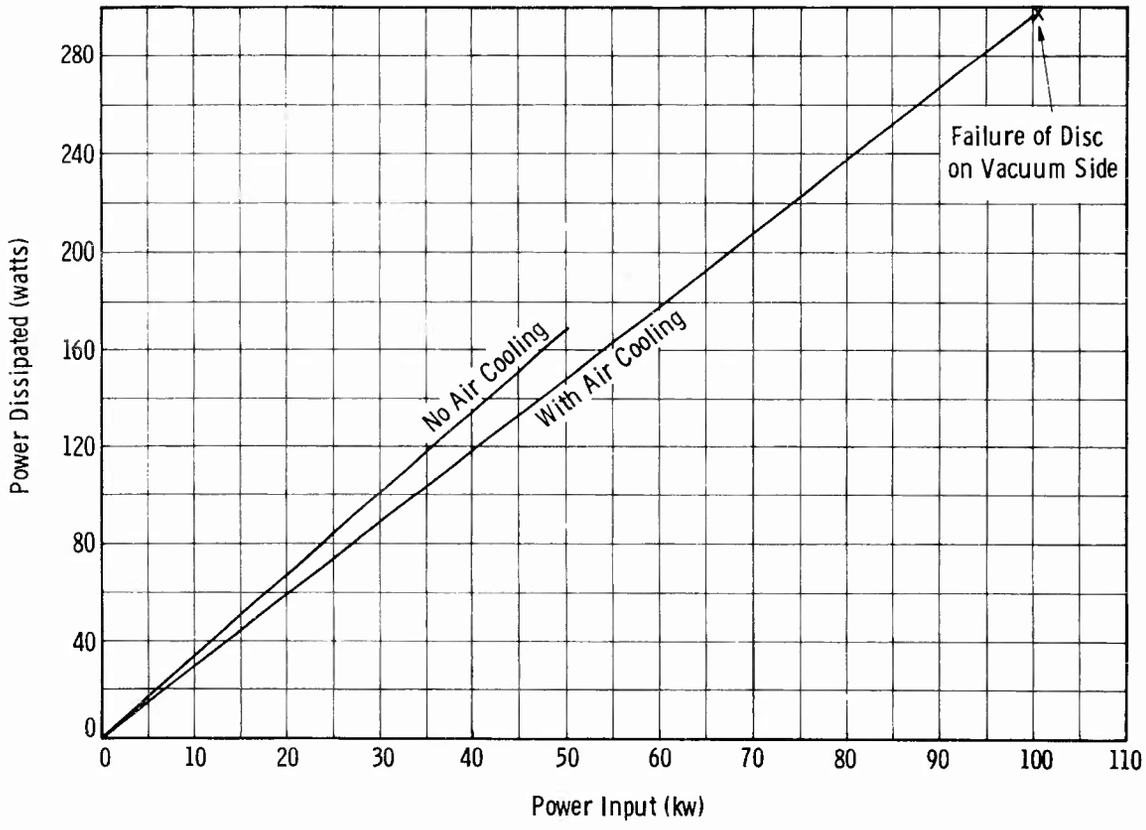

FIGURE 18
POWER DISSIPATION IN DOUBLE DISC AL300 WINDOW NO. 2
WITH ADDITIONAL AIR COOLING

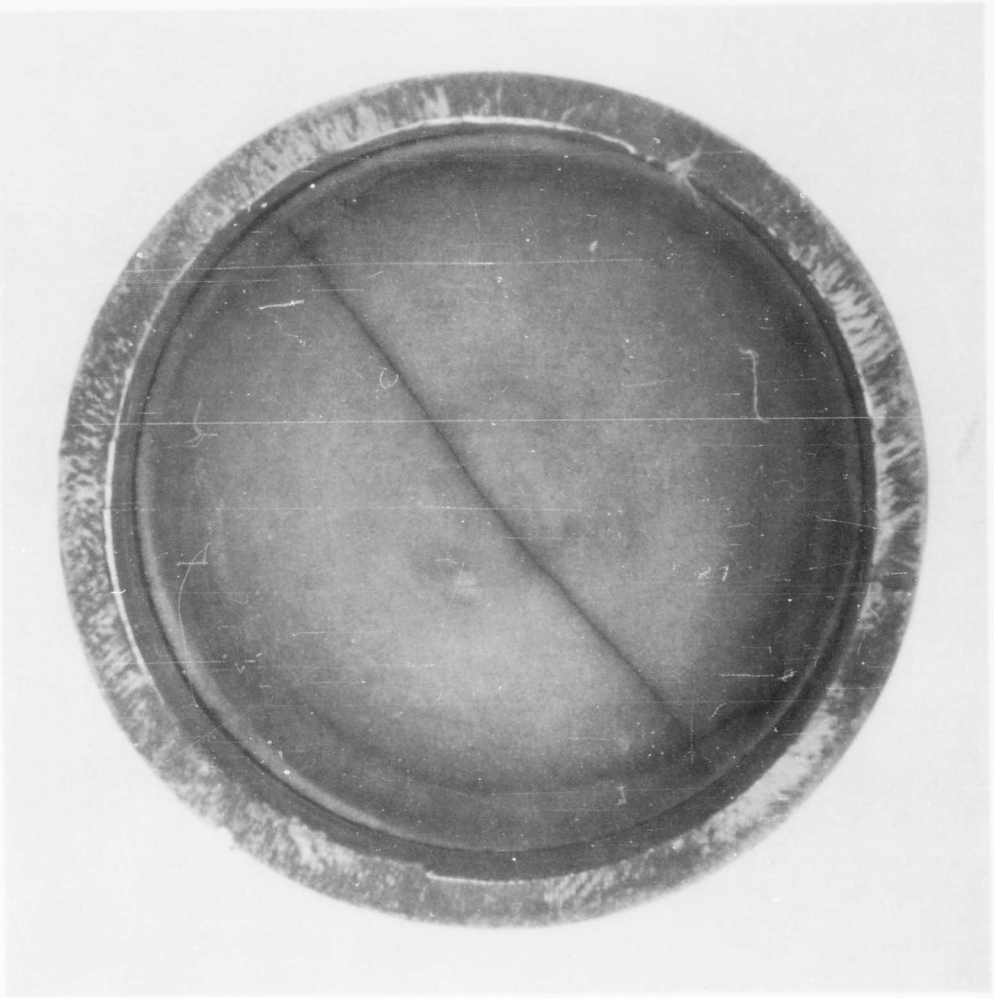

FIGURE 19
DISASSEMBLED DOUBLE DISC WINDOW NO. 2 SHOWING
FAILURE (VACUUM SIDE DISC ONLY)

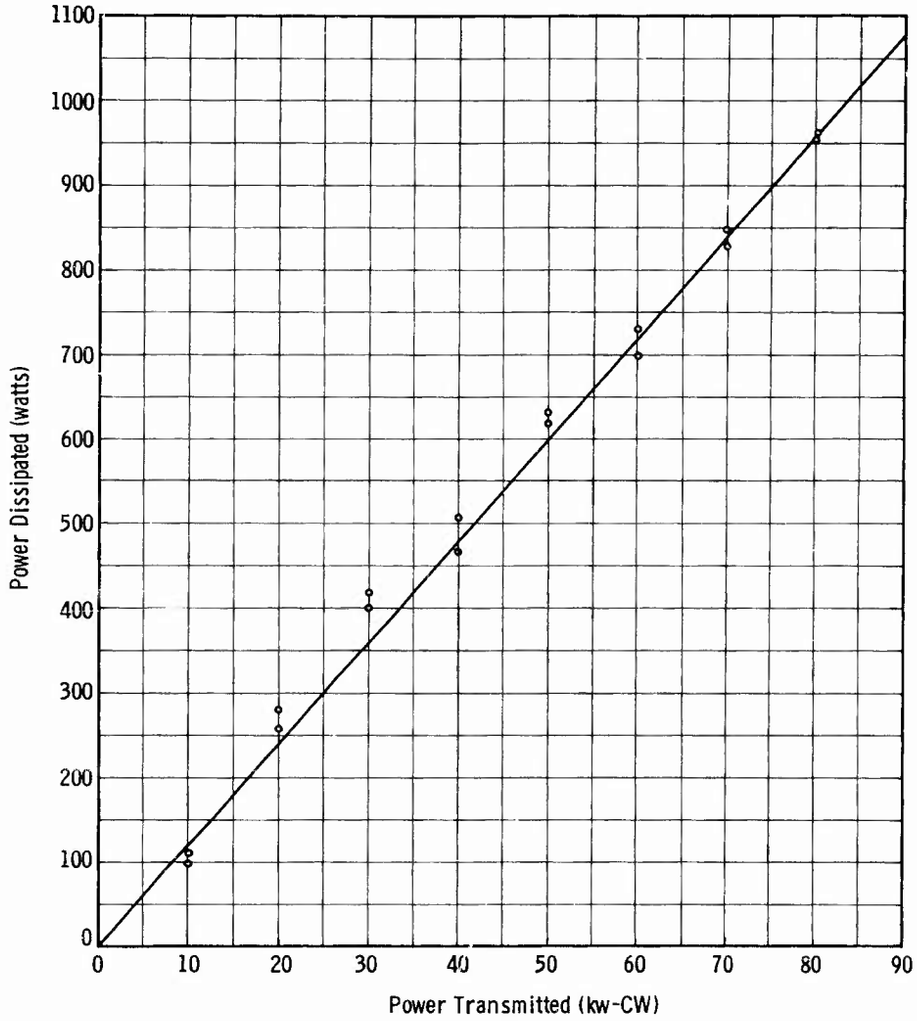

FIGURE 20
FC75 COOLED DOUBLE DISC AL400 WINDOW NO. 3

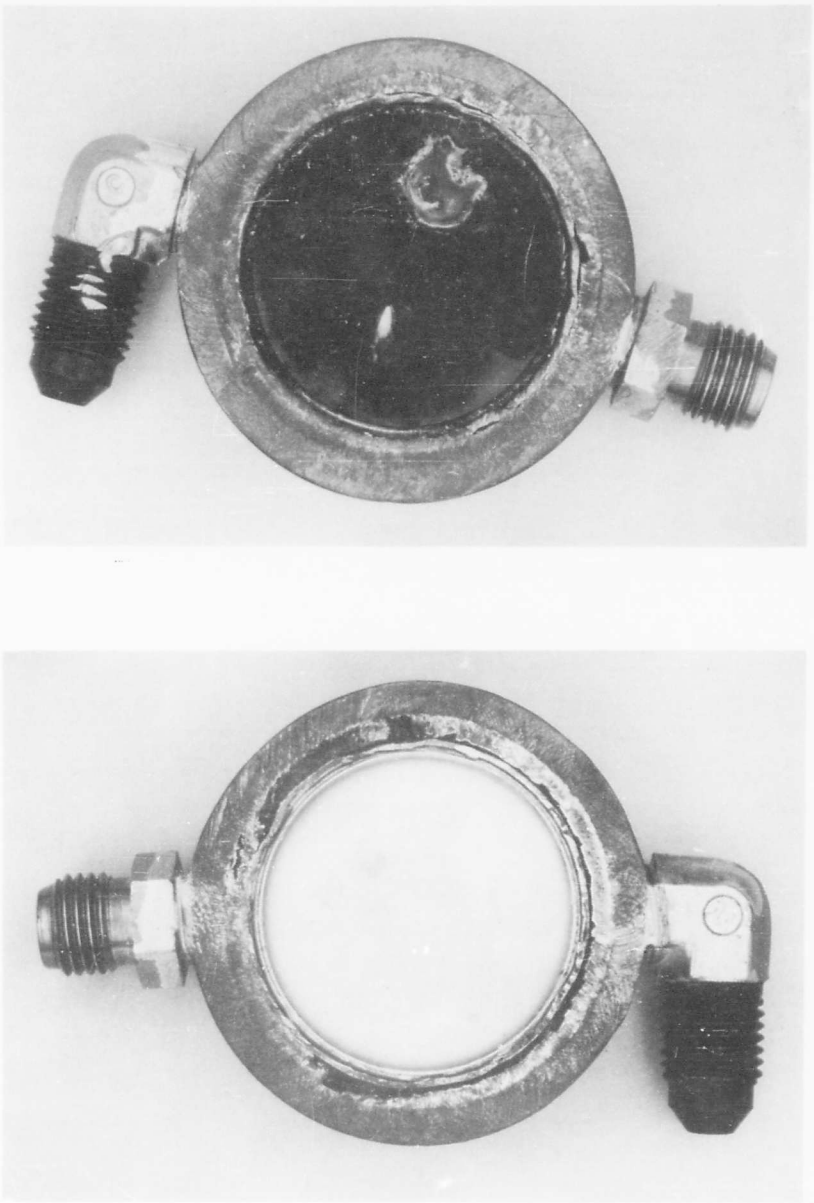

FIGURE 21
DISASSEMBLED FC75 COOLED WINDOW SHOWING HIGH TEMPERATURE FAILURE (PRESSURIZED SIDE FAILED)

D. Half-Wavelength Beryllium Oxide Windows

Testing of the broadband beryllium oxide window (dimensions as shown in Figure 4) is still in progress. As indicated in the discussion of the sapphire window, these two assemblies were connected in series to form a windowtron. The seal of the sapphire window failed at 170 kilowatts (7727 Mc), causing a temporary halt to the test. This leak was sufficiently small that a 5 liter pump could hold a 5×10^{-5} Torr vacuum. As power increased through the window, heat expansion caused the leak to become worse, until the whole evacuated region ionized at about 5×10^{-4} Torr. Before the leak was sprung the vacuum varied from 5.5×10^{-7} to 2.6×10^{-6} Torr with increasing transmitted power. The windowtron had not been baked out prior to the high power test. It is believed that bakeout will not be necessary if continual VacIon pumping is used, because cleanup of the evacuated region will be accomplished by the pumping action.

No multipactor was seen at the 170 kw level. In tests planned for the next quarter multipactor will be induced if necessary in the test windows which have been first tested to 250 kilowatts or to the limit of the ring drive power.

Figure 22 illustrates the total power lost in the windowtron including 13 inches of connecting waveguide. About 15 to 18 per cent of the loss is due to the sapphire, 25 to 35 per cent due to the beryllium oxide and the rest is in the waveguide.

E. Resonant Ring Performance

During the latter part of the third quarter, work was started to modify the resonant ring so that a longer test assembly could be tested. Until that time only single windows had been tested and the ring had been pressurized with nitrogen gas to inhibit breakdown. The maximum test length was approximately 5 inches. The new phase of work and testing with windowtrons required at least twice that length.

In order that the overall electrical length of the ring would not be increased and lead to degrading of the excellent gain characteristics, it was necessary to reduce sharply the radius of the connecting 90 degree bends. In this way several inches of test piece length were gained. In addition, another viewing port was added to enable visual monitoring of both the power input and output ends of the test window or windowtron.

A technique learned from experience with the S-band evacuated ring was also applied to the reworked X-band circuit. Each ring component was matched, if necessary, by small inductive irises, down to a VSWR of 1.02 or less. The entire ring VSWR was then checked by inserting a slotted line in place of the test section. The overall VSWR in the 7750 Mc range was also under 1.02.

Subsequent high power testing has shown that these precautionary steps have greatly improved the stability and overall performance of the resonant ring. The frequency control is now not nearly so sensitive as it had been, nor do heating effects at high power levels unbalance the circuit as readily as before.

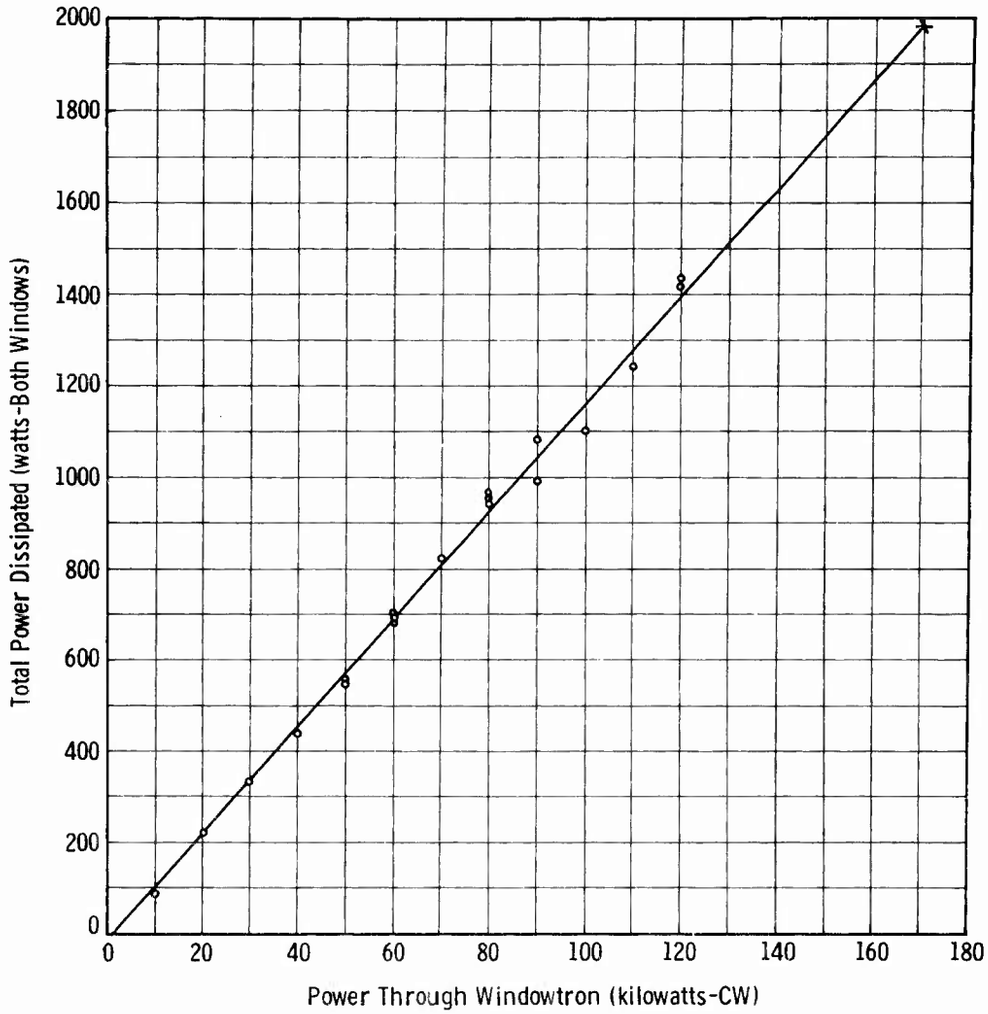

FIGURE 22
POWER DISSIPATION IN SAPPHIRE-BeO WINDOWTRON
INCLUDING 13 INCHES OF CONNECTING WAVEGUIDE

SECTION III

PROGRAM FOR NEXT QUARTER

The remaining time left to this program will be devoted largely to testing at least twelve more window assemblies. Fifteen assemblies are in preparation, but three of these are for backup purposes.

In addition to the broadband beryllium oxide window already tested to 170 kilowatts and scheduled for further testing, two similar windows are also nearing completion. The only difference in these is block length.

Two sapphire single discs are vacuum-tight and will be used to form the other half of the windowtron in which all the remaining windows will be tested to maximum power. Two single disc AL300 windows discussed in the main body of this report are also very nearly completed.

Altogether there are seven dual disc FC75 cooled aluminum oxide windows in preparation. Five of these will definitely be tested, while the remaining two will be held for use if necessary.

One dual disc beryllium oxide window is also in preparation but has not yet been brazed to a vacuum-tight cylinder. If the brazes are successful, high power testing will also be performed on it.

Once enough statistical data have been obtained from high power windowtron testing of the above windows, multipactor can be induced in the evacuated region. This will be done on the windows which have withstood maximum transmitted power and have not failed. Such a test procedure should give valuable information about the harmful effects on the dielectric and the amount of dissipated energy caused by multipactor.

SECTION IV

REFERENCES

1. Quarterly Technical Note No. 3, High Power R-F Window Study Program, RADC-TDR-63-194, furnished by Varian Associates under Contract No. AF 30(602)-2844, pp. 3-8, 33-41.

2. Ibid., pp. 16-23.

3. N. Marcuvitz, Waveguide Handbook, Radiation Laboratory Series, (New York: McGraw Hill, 1951, Vol. 10), p. 221.

4. T. Moreno, Microwave Transmission Design Data, (New York: McGraw Hill, 1948), p. 144.

5. S. Ramo and J. R. Whinnery, Fields and Waves in Modern Radio, (2nd ed.; Wiley, 1953), p. 463.

6. Quarterly Technical Note No. 3, op. cit., p. 7.

7. J. E. Storer, L. S. Sheingold and S. Stein, "A Simplified Graphical Analysis of a Two Port Waveguide Junction," Proceedings of the Institute of Radio Engineers, Vol. 41, No. 8, August 1953, pp. 1004-1013.

8. L. B. Felsen and A. A. Oliner, "Determination of Equivalent Circuit Parameters for Dissipative Microwave Structures," Proceedings of the Institute of Radio Engineers, Vol. 42, No. 2, 1954, p. 477.

9. D. B. Churchill, "High Power Waveguide Windows," Sperry Electronic Tube Division, Sperry Rand Corp., Great Neck, N. Y., Sept. 1962.

10. Quarterly Technical Note No. 2, High Power R-F Window Study Program, RADC-TDR-63-32, furnished by Varian Associates under Contract No. AF 30(602)-2844, p. 18.

11. Quarterly Technical Note No. 3, op. cit., p. 13.

12. Quarterly Technical Note No. 2, op. cit., pp. 20-23.

APPENDIX

COMPUTER PROGRAMS FOR WAVEGUIDE WINDOW SYNTHESIS

It has been shown that the computer program to synthesize waveguide windows, using the product of a multiple matrix equation, is able to predict dimensions of such windows. Actual listings of the Fortran II statements comprising this program follow, along with explanations of the use of input data and the symbols defining the parameters.

I. HALF-WAVELENGTH BLOCK WINDOW PROGRAM

A. Fortran II Statements

```
C       VARIAN ASSOCIATES
C       HIGH POWER RF WINDOW STUDY FOR RADC
C       SEVEN MATRIX SOLUTION FOR HALF WAVELENGTH BLOCK WINDOW USING
C       EQUALLY SPACED SYMMETRIC IRISES ON EACH SIDE OF CERAMIC BLOCK
C       BERYLLIUM OXIDE HALF WAVELENGTH BLOCK WINDOW
C       RELATIVE DIELECTRIC CONSTANT OF 6.5
I       DIMENSION T(2,2),S(14,2),P(2,2)
    3   READ INPUT TAPE 5,1001,A,E
 1001   FORMAT (2F7.4)
    4   WRITE OUTPUT TAPE 6,1002,A,E
 1002   FORMAT (1H1,26HWAVEGUIDE BROAD DIMENSION=,F7.4,5X,
     120HDIELECTRIC CONSTANT=,F7.4)
    5   READ INPUT TAPE 5,1003,FLO,FHI,DELTAF,DALO,DAHI,DELTDA,XLBLO,
     1XLBHI,DELTLB,XLF
 1003   FORMAT (10F6.3)
        WRITE OUTPUT TAPE 6,1004,FLO,FHI,DALO,DAHI,XLBLO,XLBHI,XLF
 1004   FORMAT (1H1,4HFLO=,F7.4,5X,4HFHI=,F7.4,5X,5HDALO=,F7.4,5X,5HDAHI=,
     1F7.4,5X,5HLBLO=,F7.4,5X,5HLBHI=,F7.4,5X,3HLF=,F7.4)
  100   N= (FHI-FLO)/DELTAF + 1.1
        DO 20 N1= 1,N
        FN1= N1-1
        FREQ= FLO + (DELTAF * FN1)
        K= (DAHI-DALO)/ DELTDA + 1.1
        DO 20 K1 = 1,K
        FK1=K1-1
        DA= DALO + (DELTDA*FK1)
        M= (XLBHI - XLBLO)/DELTLB + 1.1
        DO 20 M1= 1,M
        FM1= M1-1
        XLB= XLBLO + (DELTLB*FM1)
        C=11.80216
        XLAMDF = C/FREQ
        SFAC= (XLAMDF/(2.0*A))**2
```

```
      ROOTO= SQRTF(1.0 - SFAC)
      ROOT1= SQRTF(E - SFAC)
      PIFAC= 6.2831852/XLAMDF
      BB = PIFAC*ROOTO
      BJ = BB
      R1= ROOT1/ROOTO
      R2= ROOTO/ROOT1
      BF= PIFAC*ROOT1
      XLAMDG= XLAMDF/ROOTO
      XLAMDI = XLAMDF/ROOT1
      BLOCKL= XLAMDI/2.0
      PI = 3.1415926
C     COMPUTE SUSCEPTANCE VALUES FOR WR112 WAVEGUIDE
      ARG1=(PI*DA)/(2.0*A)
      COT = (COSF(ARG1))/(SINF(ARG1))
      SFAC2=((0.66667*A)/XLAMDF)**2
      ROOT2= SQRTF(1.0-SFAC2)
      CORFAC= 1.0 + ((0.75/ROOT2) -0.75)*(SINF(PI*DA/A))**2
      SUSNOR=(COT**2)/CORFAC
      SUS= (SUSNOR*XLAMDG)/A
      Y1 = SUS/2.0
C     COMPUTE COEFFICIENTS OF MATRICES FOR RECTANGULAR BLOCK WINDOW
      S(1,1) = 1.0
      S(2,2)= 1.0
      S(1,3)= Y1
      S(1,4)= Y1
      S(2,3)= -Y1
      S(2,4)= -Y1
      S(3,1)= COSF(XLB*BB)
      S(4,2) = S(3,1)
      S(3,3)= -SINF(XLB*BB)
      S(4,4)= -S(3,3)
      S(5,1)= 0.5*(1.0 + R1)
      S(6,2)= S(5,1)
      S(5,2)= 0.5*(1.0 -R1)
      S(6,1) = S(5,2)
      S(7,1) = COSF(XLF*BF)
      S(8,2) = S(7,1)
      S(7,3) = -SINF(XLF*BF)
      S(8,4) = -S(7,3)
      S(9,1) = 0.5*(1.0 + R2)
      S(10,2) = S(9,1)
      S(9,2) = 0.5*(1.0 - R2)
      S(10,1) = S(9,2)
      S(11,1) = S(3,1)
      S(12,2) = S(11,1)
      S(11,3) = S(3,3)
      S(12,4) = -S(11,3)
      S(13,1) = 1.0
      S(14,2) = 1.0
```

```
      S(13,3) = Y1
      S(13,4) = Y1
      S(14,3) = -Y1
      S(14,4) = -Y1
 1005 FORMAT (1H ,2F20.8,15X,2F20.8)
C     MULTIPLY COMPLEX MATRICES
      WRITE OUTPUT TAPE 6, 1006
 1006 FORMAT (1HO,40HCOEFFICIENTS AFTER MATRIX MULTIPLICATION)
I     T(1,1)= (1.0,0.0)
I     T(1,2)= (0.0,0.0)
I     T(2,1)= (0.0,0.0)
I     T(2,2)= (1.0,0.0)
      DO 10  J=1,13,2
I     P(1,1)= T(1,1)*S(J,1) + T(1,2)*S(J+1,1)
I     P(1,2)= T(1,1)*S(J,2) + T(1,2)*S(J+1,2)
I     P(2,1)= T(2,1)*S(J,1) + T(2,2)*S(J+1,1)
I     P(2,2)= T(2,1)*S(J,2) + T(2,2)*S(J+1,2)
I     T(1,1) = P(1,1)
I     T(1,2) = P(1,2)
I     T(2,1)= P(2,1)
I  10 T(2,2)= P(2,2)
      WRITE OUTPUT TAPE 6,1005,T(1,1),T(1,3),T(1,2),T(1,4),
     1                         T(2,1),T(2,3),T(2,2),T(2,4)
      RHO= SQRTF((T(2,1)**2 + T(2,3)**2)/(T(2,2)**2 + T(2,4)**2))
      VSWR= (1.0 + RHO)/(1.0 - RHO)
   20 WRITE OUTPUT TAPE 6,1007,FREQ,DA,XLB,VSWR,BLOCKL,SUSNOR,SUS
10070FORMAT (1HO,5X,4HWITH,5X,5HFREQ=,F5.2,5X,3HDA=,F6.4,5X,3HLB=,F6.4,
     15X,5HVSWR=,F8.5,5X,7HBLOCKL=,F7.5,5X,7HSUSNOR=,F6.4,5X,4HSUS=,
     2F6.4)
      GO TO 5
      END
*     DATA
```

B. Input Data Definitions

A = broad dimension of waveguide

E = relative dielectric constant of the ceramic

FLO = low end of frequency range

FHI = high end of frequency range

DELTAF = increment of frequency

DALO = iris gap width minimum

DAHI = iris gap width maximum

DELTDA = iris gap width increment

XLBLO = minimum distance between iris and window face

XLBH = maximum distance between iris and window face

DELTLB = incremental distance between iris and face of window

XLF = thickness of window used

In this example, only two input data cards have been used, and each has been read by separate "read" statement. However, before the computer goes to the "end" statement and shuts off, it will return to statement 5 to check whether additional data cards are available. In this way several completely different windows can be run provided the same size waveguide is used and the dielectric constant has not changed.

The input dimension ranges of iris gap size, spacing between iris and window and frequency range will generally be known by the designer to some approximation. This is all that is necessary to be given to the computer.

C. Symbol Definitions

C = velocity of light in inches per second

XLAMDF = free space wavelength

Since the term $\sqrt{\epsilon_R - \left(\frac{\lambda}{2a}\right)^2}$ shows up in several places, it is given the name of ROOT 1 and is used to calculate

$$R_1 = \frac{\sqrt{\epsilon_R - \left(\frac{\lambda o}{2a}\right)^2}}{\sqrt{1 - \left(\frac{\lambda o}{2a}\right)^2}} \qquad \text{and } \beta f = \frac{2\pi}{\lambda o} \sqrt{\epsilon_R - \left(\frac{\lambda o}{2a}\right)^2}$$

where

$$\left(\frac{\lambda o}{2a}\right)^2 = \text{SFAC}$$

$$\sqrt{1 - \left(\frac{\lambda o}{2a}\right)^2} = \text{ROOTO} = \text{SQRTF (1.0-SFAC)}$$

$$\frac{2\pi}{\lambda o} = \text{PIFAC}$$

and β_f = PIFAC * ROOT 1

Equation (1), page 3, is similarly broken up into components and defined. In the calculation of the shunt sesceptance values,

$$\frac{\pi d}{2a} = \text{ARGI}$$

$$\left(\frac{2a}{3\lambda}\right)^2 = \text{SFAC2}$$

$$\sqrt{1 - \left(\frac{2a}{3\lambda}\right)^2} = \text{ROOT2}$$

$$\text{DA} = \text{iris gap width}$$

$$1 + 3/4 \left\{ \frac{1}{\sqrt{1 - \left(\frac{2a}{3\lambda}\right)^2}} - 1 \right\} \sin^2 \frac{\pi d}{a} = \text{CORFAC}$$

$$\frac{B}{Y_o} = \text{SUS}$$

$$\frac{B}{Y_o} \frac{a}{\lambda g} = \text{SUSNOR}$$

$$\frac{B}{2Y_o} = Y$$

also

$$\beta_b = \text{BB}$$

$$\beta_j = \text{BJ}$$

$$\beta_f = \text{BF}$$

II. THIN DISC WINDOW PROGRAM

The computer program for thin disc windows is very much like its counterpart for block windows. However, this one was compiled for an eleven matrix equation allowing computation for double thin disc windows with dielectric coolant between discs. Many of the variable names are also the same. The input data for the scattering matrix

of T^a are in terms of a magnitude and an angle as measured. The computer puts it in the complex form of

$$W(1) = AMP11 * COSF(THET11)$$

which is the real part of S_{11}. The values of both the scattering matrices and the transmission parameters are printed out along with the desired impedance match information.

A. Fortran II Statements

```
*      WAVEGUIDE WINDOW SYNTHESIS FOR FLOYD JOHNSON VARIAN JO 19094
*      XEQ
*      LABEL
CTDWSYN    ELEVEN MATRIX SOLUTION FOR SYMONS TYPE THIN DISC WINDOW
C          IN FORTRAN 2 LANGUAGE
C      WINDOW STUDY R.A.D.C
C      ALUMINUM OXIDE RELATIVE DIELECTRIC CONSTANT OF 9.34
I      DIMENSION T(2,2),S(22,2),P(2,2)
       DIMENSION W1(2),W2(2),W3(2)
    3  READ INPUT TAPE 5,1001,D1,D2,E1,E2
 1001  FORMAT (4F7.4)
    4  WRITE OUTPUT TAPE 6,1002,D1,D2,E1,E2
 1002  FORMAT (1H1,3HD1=,F6.3,5X,3HD2=,F6.3,5X,3HE1=,F6.3,5X,3HE2=,F6.3)
       READ INPUT TAPE 5,1013,XLBLO,XLBHI,DELTLB,XLDLO,XLDHI,DELTLD
 1013  FORMAT (6F7.4)
       WRITE OUTPUT TAPE 6,1014,XLBLO,XLBHI,DELTLB,XLDLO,XLDHI,DELTLD
 1014  FORMAT (1H0,5HLBLO=,F6.3,5X,5HLBHI=,F6.3,5X,7HDELTLB=,F6.3,5X,
     15HLDLO=,F6.3,5X,5HLDHI=,F6.3,5X,7HDELTLD=,F6.3)
       READ INPUT TAPE 5,1013,XLFLO,XLFHI,DELTLF,XLHLO,XLHHI,DELTLH
       WRITE OUTPUT TAPE 6,1015,XLFLO,XLFHI,DELTLF,XLHLO,XLHHI,DELTLH
 1015  FORMAT (1H0,5HLFLO=,F6.3,5X,5HLFHI=,F6.3,5X,7HDELTLF=,F6.3,5X,
     15HLHLO=,F6.3,5X,5HLHHI=,F6.3,5X,7HDELTLH=,F6.3)
    5  READ INPUT TAPE 5,1003,FREQ,AMP11,THET11,AMP12,THET12,AMP22,THET22
 1003  FORMAT (7F7.4)
    6  WRITE OUTPUT TAPE 6,1004,FREQ,AMP11,THET11,AMP12,THET12,AMP22,
     1THET22
 1004  FORMAT (1H1,5HFREQ=,F5.2,5X,6HAMP11=,F7.4,5X,7HTHET11=,F7.4,5X,
     16HAMP12=,F7.4,5X,7HTHET12=,F7.4,5X,6HAMP22=,F7.4,5X,7HTHET22=,
     2F7.4)
       W1(1)= AMP11*COSF(THET11)
       W1(2)= AMP11*SINF(THET11)
       W2(1)= AMP12*COSF(THET12)
       W2(2)= AMP12*SINF(THET12)
       W3(1)= AMP22*COSF(THET22)
  150  W3(2)= AMP22*SINF(THET22)
   25  WRITE OUTPUT TAPE 6,1011
 1011  FORMAT (1H0,49H ABRUPT TRANSITION SCATTERING MATRIX COEFFICIENTS)
   30  WRITE OUTPUT TAPE 6,1008,W1(1),W1(2),W2(1),W2(2),W3(1),W3(2)
 1008  FORMAT (1H ,5X,6HW1(1)=,F9.5,5X,6HW1(2)=,F9.5,5X,6HW2(1)=,F9.5,
```

```
     15X,6HW2(2)=,F9.5,5X,6HW3(1)=,F9.5,5X,6HW3(2)=,F9.5)
I      S(1,1)= W2 - (W1*W3/W2)
I      S(1,2)= W3/W2
I      S(2,1)= -W1/W2
I      S(2,2)= (1.0,0.0)/W2
   40 WRITE OUTPUT TAPE 6,1009
 1009 FORMAT (1HO,5X,42H ABRUPT TRANSITION TRANSMISSION PARAMETERS)
   50 WRITE OUTPUT TAPE 6,1010,S(1,1),S(1,3),S(1,2),S(1,4),
     1                         S(2,1),S(2,3),S(2,2),S(2,4)
 1010 FORMAT (1H ,2F20.8,15X,2F20.8)
      C=11.80216
      XLAMDA= C/FREQ
      RFAC1 = (0.58612*XLAMDA/D1)**2
      RFAC2 = (0.58612*XLAMDA/D2)**2
      ROOT1 = SQRTF(1.0-RFAC1)
      ROOT2 = SQRTF(E1-RFAC1)
      ROOT3 = SQRTF(E2-RFAC2)
      PIFAC= 6.2831852/XLAMDA
      BB= PIFAC*ROOT1
      BD= PIFAC*ROOT2
      BF= PIFAC*ROOT3
      BJ = BB
      BH = BD
      R1= ROOT2/ROOT1
      R2= ROOT3/ROOT2
      R3= ROOT2/ROOT3
      R4= ROOT1/ROOT2
C     COMPUTE COEFFICIENTS OF MATRICES FOR THIN DISC WINDOWS
      S(5,1) = 0.5*(1.0 + R1)
      S(6,2) = S(5,1)
      S(5,2) = 0.5*(1.0 - R1)
      S(6,1) = S(5,2)
      S(9,1) = 0.5*(1.0 + R2)
      S(10,2)= S(9,1)
      S(9,2) = 0.5*(1.0 - R2)
      S(10,1)= S(9,2)
      S(13,1)= 0.5*(1.0 + R3)
      S(14,2)= S(13,1)
      S(13,2)= 0.5*(1.0 - R3)
      S(14,1)= S(13,2)
      S(17,1)= 0.5*(1.0 + R4)
      S(18,2)= S(17,1)
      S(17,2)= 0.5*(1.0 - R4)
      S(18,1)= S(17,2)
I     S(21,1) = S(1,1)
I     S(21,2) = -S(2,1)
I     S(22,1) = -S(1,2)
I     S(22,2) = S(2,2)
  100 K=(XLBHI - XLBLO)/DELTLB + 1.1
```

```
      DC 20 K1= 1,K
      FK1=K1-1
      XLB= XLBLO + (DELTLB*FK1)
      XLJ = XLB
      S(3,1) =COSF(XLB*BB)
      S(4,2) = S(3,1)
      S(3,3) = -SINF(XLB*BB)
      S(4,4) = -S(3,3)
      S(19,1)= S(3,1)
      S(20,2)= S(19,1)
      S(19,3) = S(3,3)
      S(20,4)= -S(19,3)
      L= (XLDHI - XLDLO)/DELTLD + 1.1
      DC 20  L1=1,L
      FL1= L1-1
      XLD= XLDLO + (DELTLD*FL1)
      S(7,1) = COSF(XLD*BD)
      S(8,2) = S(7,1)
      S(7,3) = -SINF(XLD*BD)
      S(8,4) = -S(7,3)
      M= (XLFHI - XLFLO)/DELTLF + 1.1
      DC 20 M1=1,M
      FM1= M1-1
      XLF= XLFLO + (DELTLF*FM1)
      S(11,1)= COSF(XLF*BF)
      S(12,2)= S(11,1)
      S(11,3)= -SINF(XLF*BF)
      S(12,4)= -S(11,3)
      N= (XLHHI - XLHLO)/DELTLH + 1.1
      DC 20 N1=1,N
      FN1= N1-1
      XLH= XLHLO + (DELTLH*FN1)
      S(15,1)= COSF(XLH*BH)
      S(16,2)= S(15,1)
      S(15,3)=-SINF(XLH*BH)
      S(16,4)= -S(15,3)
C     MULTIPY COMPLEX MATRICES
      WRITE OUTPUT TAPE 6,1006
 1006 FORMAT (1H0,41H COEFFICIENTS AFTER MATRIX MULTIPLICATION)
I     T(1,1) = (1.0,0.0)
I     T(1,2) = (0.0,0.0)
I     T(2,1) = (0.0,0.0)
I     T(2,2) = (1.0,0.0)
      DC 10 J=1,21,2
I     P(1,1) = T(1,1)*S(J,1) + T(1,2)*S(J+1,1)
I     P(1,2) = T(1,1)*S(J,2) + T(1,2)*S(J+1,2)
I     P(2,1) = T(2,1)*S(J,1) + T(2,2)*S(J+1,1)
I     P(2,2) = T(2,1)*S(J,2) + T(2,2)*S(J+1,2)
I     T(1,1)=P(1,1)
I     T(1,2)=P(1,2)
```

```
I       T(2,1)=P(2,1)
I    10 T(2,2)=P(2,2)
        WRITE OUTPUT TAPE 6,1005,T(1,1),T(1,3),T(1,2),T(1,4),
       1                         T(2,1),T(2,3),T(2,2),T(2,4)
 1005   FORMAT (1H ,2F20.8,15X,2F20.8)
        RHO = SQRTF((T(2,1)**2+T(2,3)**2)/ (T(2,2)**2+T(2,4)**2))
        VSWR = (1.0+RHO)/(1.0-RHO)
    20  WRITE OUTPUT TAPE 6,1007,XLB,XLD,XLF,XLH,VSWR
 1007   FORMAT (1HO,5X,4HWITH,5X,3HLB=,F6.4,5X,3HLD=,F6.4,5X,3HLF=,F6.4,
       15X,3HLH=,F6.4,5X,5HVSWR=,F8.5)
        GO TO 5
        END
*       DATA
```

B. Input Data Definitions

D1 = diameter of cylinder

D2 = reduced diameter of cylinder (as when using supporting hoops)

E1 = relative dielectric constant of ceramic window

E2 = relative dielectric constant of dielectric coolant

XLB, XLD, XLF, XLH and XLJ are all waveguide section lengths.

S(1, 1) is the computer notation for T_{11} etc.

W1 = W1(1) + jW1(2).

DISTRIBUTION LIST

Copy No.	No. of Copies	Address
1	1	**RADC (RALTP, ATTN: D. Bussey) Griffiss AFB NY
2	1	*RADC (RAAPT) Griffiss AFB NY
3	1	*RADC (RAALD) Griffiss AFB NY
4	1	*GEEIA (ROZMCAT) Griffiss AFB NY
5	1	*RADC (RAIS, ATTN: Mr. Malloy) Griffiss AFB NY
6	1	US Army Electronics R and D Labs Liaison Officer RADC, Griffiss AFB NY
7	1	*AUL (3T) Maxwell AFB Ala
8	1	ASD (ASAPRD) Wright-Patterson AFB Ohio
9	1	Chief, Naval Research Lab ATTN: Code 2027 Wash 25 DC
10	1	Air Force Field Representative Naval Research Lab ATTN: Code 1010 Wash 25 DC
11	1	Commanding Officer USASRDL ATTN: SIGRA/SL-ADT Ft Monmouth NJ
12	1	National Aeronautics and Space Admin Langley Research Center Langley Station Hampton Virginia ATTN: Librarian
13	1	Central Intelligence Agency ATTN: OCR Mail Room 2430 E Street NW Wash 25 DC
14	1	US Strike Command ATTN: STRJ5-OR Mac Dill AFB Fla
15	1	AFSC (SCSE) Andrews AFB Wash 25 DC
16	1	Commanding General US Army Electronic Proving Ground ATTN: Technical Documents Library Ft Huachuca Ariz
17 - 26	10	DDC (TISIA-2) Cameron Station Alexandria, Va., 22314
27	1	AFSC (SCFRE) Andrews AFB Wash 25 DC
28	1	Hq USAF (AFCOA) Wash 25 DC
29	1	AFOSR (SRAS/Dr. G. R. Eber) Holloman AFB NMex
30	1	Office of Chief of Naval Operations (Op-724) Navy Dept Wash 25 DC
31	1	Commander US Naval Air Dev Cen (NADC Lib) Johnsville Pa
32	1	Commander Naval Missile Center Tech Library (Code NO 3022) Pt Mugu Calif
33	1	Bureau of Naval Weapons Main Navy Bldg Wash 25 DC ATTN: Technical Librarian, DL1-3
34	1	Redstone Scientific Information Center US Army Missile Command Redstone Arsenal, Alabama
35	1	Commandant Armed Forces Staff College (Library) Norfolk 11 VA
36	1	ADC (ADOAC-DL) Ent AFB Colo
37	1	AFFTC (FTOOT) Edwards AFB Calif
38	1	Commander US Naval Ordnance Lab (Tech Lib) White Oak, Silver Springs Md
39	1	Commanding General White Sands Missile Range New Mexico ATTN: Technical Library
40	1	Director US Army Engineer R and D Labs Technical Documents Center Ft Belvoir VA
41	1	ESD (ESRL) L G Hanscom Fld Bedford Mass
42	1	Commanding Officer and Director US Navy Electronics Lab (LIB) San Diego 52 Calif
43	1	ESD (ESAT) L G Hanscom Fld Bedford Mass
44	1	Commandant US Army War College (Library) Carlisle Barracks Pa
45	1	APGC (PGAPI) Eglin AFB Fla
46	1	AFSWC (SWOI) Kirtland AFB NMex
47	1	Dr. A. Pronner Litton Industries 960 Industrial Road San Carlos Calif
48	1	Mr. Del Churchill Sperry Gyroscope Co Great Neck NY
49	1	ARPA ATTN: Col Lindsay Washington 25 DC
50	1	RTD (RTGS) Bolling AFB Washington 25 DC
51	1	Dr. Louis R. Bloom Sylvania Elect Prod Inc Physics Lab 208-20 Willetts Point Blvd Bayside, Long Island NY

*Mandatory

**Project Engineer will enter his symbol and name in the space provided.

DISTRIBTUION LIST (Cont.)

Copy No.	No. of Copies	Address
52 - 53	2	Technical Library Varian Associates 611 Hansen Way Palo Alto, California
54	1	Dr. L. A. Roberts Watkins Johnson Co Palo Alto, California
55	1	Mr. Gerald Klein, Mgr Microwave Tube Section Applied Research Dept Westinghouse Elect Corp Friendship Intl Airport Box 746 Baltimore, Md.
56	1	Hughes Aircraft Co Culver City, Calif ATTN: Everett M. Wallace
57	1	Bendix Aviation Corp Red Bank Division Eatontown, New Jersey ATTN: John Johnstone
58 - 59	2	Eitel Mc Cullough Inc 901 Industrial Way San Carlos, California ATTN: Stella R. Vetter Research Library
60	1	Mr. F. E. Ferrira Director of Research Coors Porcelain Co Golden, Colorado
61 - 62	2	Mr. M. Hoover RCA Lancaster, Pa
63	1	Dr. D. Goodman Sylvania Microwave Tube Lab 500 Evelyn Avenue Mt. View, California
64	1	Mr. A. E. Harrison University of Washington Dept of Elect Engineering Seattle 5, Washington
65	1	Mr. Shelden S. King Eng Librarian Westinghouse Elect Corp PO Box 284 Elmira, New York
66	1	Kane Engineering Labs 845 Commercial Street Palo Alto, California ATTN: Mr. F. Kane
67	1	Electrical Industries Co Murray Hill, New Jersey ATTN: Mr. Peter A. Muto
68	1	Mr. L. E. Gates, Jr. 20/1365 41-48-20 Hughes Aircraft Co Culver City, California
69	1	Mr. Theodore Poumbanis Microwave Elect Prod Inc Microwave Device Operations 600 Evelyn Avenue Mountain View, California
70	1	Dr. R. G. E. Hutter Sylvania Microwave Tube Lab 500 Evelyn Ave Mt. View, California
71	1	Dr. William Watson Litton Industries 960 Industrial Road San Carlos, Calif
72	1	Technical Library Litton Industries 960 Industrial Road San Carlos, Calif
73	1	Mr. Ted Moreno Varian Associates 611 Hansen Way Palo Alto, Calif
74	1	Mr. C. Dalman Cornell University Dept of Elect Eng Ithaca, New York
75	1	Mr. Donald Priest Eitel-Mc Cullough Inc San Bruno, California
76	1	Mr. T. Marchese Federal Tele Labs Inc 500 Washington Ave Nutley, New Jersey
77	1	Mr. S. Webber General Elect Microwave Lab 601 California Ave Palo Alto, California
78	1	Mr. Lester Firestein Stanford Research Institute Palo Alto, California
79	1	Dr. D. D. King Johns Hopkins University Radiation Laboratory Baltimore 2, Maryland
80	1	Mr. R. Butman M.I.T. Lincoln Laboratory PO Box 73 Lexington 73, Mass.
81	1	Dr. S. F. Kaisel Microwave Electronics Corp 4061 Transport Street Palo Alto, California
82	1	Ohio State University Dept of Elect Engineering Columbus 10, Ohio ATTN: Prof. E. M. Boone
83	1	Mr. W. C. Brown Spencer Lab Raytheon Mfg Co Wayside Rd Burlington, Mass.
84	1	Mr. W. Teich Raytheon Mfg Co Spencer Lab Burlington, Mass.
85	1	Mr. Hans Jenny RCA Elect Tube Div 415 South 5th Street Harrison, New Jersey
86	1	Mr. P. Bergman Sperry Corp Elect Tube Div Gainesville, Florida
87	1	Dr. M. Chodorow Stanford University Microwave Lab Stanford, California
88	1	Dr. Bernard Arfin Varian Associates 611 Hansen Way Palo Alto, California
89	1	Dept of Electrical Eng University of Florida Gainsville, Florida
90	1	Dr. E. D. Mc Arthur General Elect Co Electron Tube Div of Research Lab The Knolls Schenectady, New York
91	1	Mr. J. T. Milek Hughes Aircraft Co Electron Tube Laboratory Culver City, California
92	1	University of Illinois Electrical Eng Research Lab Urbana, Ill ATTN: Technical Editor

DISTRIBUTION LIST (Cont.)

Copy No.	No. of Copies	Address
93	1	Dr. Norman Moore Litton Industries 960 Industrial Road San Carlos, California
94	1	Mass Institute of Technology Research Laboratory of Electronics Cambridge 39, Mass. ATTN: Document Library
95	1	University of Minnesota Minneapolis, Minnesota ATTN: Dr. W. G. Shepherd Dept of Elect Eng
96	1	Dr. M. Ettinberg, Polytechnic Institute of Brooklyn Microwave Research Inst Brooklyn 1, New York
97	1	Mr. John M. Osepchuk Raytheon Co Spencer Lab Burlington, Mass
98	1	Dr. Bernard Hershenon RCA Labs Princeton, New Jersey
99	1	Dr. W. M. Webster Director Electronic Research Lab RCA Labs Princeton, New Jersey
100	1	Stanford University Elect Research Laboratory Stanford, California ATTN: Mr. D. C. Bacon Asst Director
101	1	Dr. D. A. Watkins Stanford University Electronics Laboratory Stanford, California
102	1	Secretariat Advisory Group on Electron Tubes 346 Broadway New York 13, New York
103	1	Bell Telephone Labs Murry Hill Laboratory Murry Hill, New Jersey ATTN: Dr. J. R. Pierce
104	1	Mr. A.G. Peifer Research Laboratories Div The Bendix Corporation Southfield Detroit, Michigan
105	1	Professor R. M. Saunders University of California Dept of Engineering Berkeley 4, California
106 - 107	2	Commanding Officer US Army Signal R and D Lab ATTN: Logistics Div (SIGRA/SL-PRT) L. N. Heynick Ft. Monmouth New Jersey
108	1	Field Emession Corp. 611 Third Street McMinnville Oregon ATTN: Mr. F. M. Charbonnier
109	1	Dr. Robert T. Young Chief Electron Tube Branch Diamond Ord Fuse Lab Washington 25, D.C.
110	1	Applied Radiation Co Walnut Creek California ATTN: Mr. Niel J. Norris
111	1	RTD (RTH) Bolling AFB Washington 25, D.C.
112	1	The Electronics Research Lab 427 Cory Hall The University of California Berkeley 4, California ATTN: Mrs. Simmons
113	1	Professor W. G. Worcester University of Colorado Dept of Electrical Engineering Boulder, Colorado
114	1	Columbia University Columbia Radiation Lab 538 W 120th Street New York 27, N.Y.
115	1	NAFEC Library Bldg. 3 Atlantic City, N. J.
116 - 119	4	RADC(RALTP, Attn: D. Bussey) GRIFFISS AFB, N. Y.
120	1	AFMTC Tech. Library (MU-135) Patrick AFB, Fla.
121	1	AFMTC (MTBAT) Patrick AFB, Fla.
122	1	Sidney J. Stein Electro-Science Labs. Inc. 1133-35 Arch Street Philadelphia 7, Pa.
123 - 140	18	Retained by Varian Associates

UNCLASSIFIED